WCAP 11774

TECHNICAL BASES FOR ELIMINATING RESIDUAL HEAT REMOVAL (RHR) LINE RUPTURE FROM THE STRUCTURAL DESIGN BASIS FOR SOUTH TEXAS PROJECT UNITS 1 AND 2

June 1988

B. J. Coslow
S. A. Swamy
F. J. Witt
Y. S. Lee

Verified by: _J̶o̶h̶n̶ ̶C̶.̶ ̶S̶c̶h̶m̶e̶r̶t̶z̶_
J. C. Schmertz

Approved by: _____
S. S. Palusamy, Manager
Structural Materials Engineering

Work Performed Under Shop Order TREJ-950

WESTINGHOUSE ELECTRIC CORPORATION
Power Systems Division
P.O. Box 2728
Pittsburgh, Pennsylvania 15230-2728

TABLE OF CONTENTS

TABLE OF CONTENTS (Cont'd.)

TABLE OF CONTENTS (Cont'd.)

LIST OF TABLES

LIST OF TABLES (Cont'd.)

LIST OF FIGURES

LIST OF FIGURES (Cont'd.)

SECTION 1.0

INTRODUCTION

1.1 Background

The current structural design basis for the RHR line requires postulating non-mechanistic circumferential and longitudinal pipe breaks. This results in additional plant hardware (e.g. pipe whip restraints and jet shields) which would mitigate the dynamic consequences of the pipe breaks. It is, therefore, highly desirable to be realistic in the postulation of pipe breaks for these lines, and thereby eliminate the need for some of the plant hardware. Presented in this report are the descriptions of a mechanistic pipe break evaluation method and the analytical results that are used for establishing that a circumferential type break will not occur. The evaluations considering circumferentially oriented flaws envelop longitudinal cases, as discussed in section 1.2. As-built loads are used in the evaluation.

1.2 Scope and Objective

The purpose of this investigation is to demonstrate leak-before-break for the high energy portion of the RHR line. The piping covered by this evaluation is shown in figure 1-1, and includes the high energy piping from the primary loop junction up to the first isolation valve. Down stream of the isolation valve, the piping is classified as moderate energy piping. Schematic drawings of the piping system are shown in section 5.0. The recommendations and criteria proposed in NUREG 1061 Volume 3 (1-1) are used in this evaluation. These criteria and resulting steps of the evaluation procedure can be briefly summarized as follows:

1) Calculate the applied loads. Identify the location at which the highest stress occurs.

2) Identify the materials and the associated material properties.

1-1

3) Postulate a surface flaw at the governing location with the least favorable combination of stress and material properties. Determine fatigue crack growth. Show that a through-wall crack will not result.

4) Postulate a through-wall flaw at the governing location. The size of the flaw should be large enough so that the leakage is assured of detection with margin using the installed leak detection equipment when the pipe is subjected to normal operating loads. A margin of 10 is demonstrated between the calculated leak rate and the leak detection capability. The associated flaw is called the leakage size flaw.

5) Using normal plus SSE loads, demonstrate that there is a margin of at least 2 between the leakage size flaw and the critical size flaw.

6) Review the operating history to ascertain that operating experience has indicated no particular susceptibility to failure from the effects of corrosion, water hammer or low and high cycle fatigue.

7) For the base and weld metals actually in the plant provide the material properties including toughness and tensile test data. Justify that the properties used in the evaluation are representative of the plant specific material. Evaluate long term effects such as thermal aging where applicable.

8) Demonstrate margin of at least 1.4 on applied load for the leakage size flaw.

The flaw stability criteria used in this analysis address both the global and local stability for a postulated through-wall circumferential flaw. The global analysis is carried out using the [$]^{a,c,e}$ method, based on traditional plastic limit load concepts, but accounting for [$]^{a,c,e}$ and taking into account the presence of a flaw (1-1).

The local stability analysis is carried out using elastic-plastic fracture mechanic analysis procedures. In this report the EPRI elastic-plastic fracture handbook (1-2) method was used for the local stability analysis.

The leak rate is calculated for the as-built normal operating condition. The leak rate prediction model used in this evaluation is an [

$]^{a,c,e}$ The crack opening area required for calculating the leak rates is obtained by subjecting the postulated through-wall flaw to normal operating loads (1-3). Surface roughness is accounted for in determining the leak rate through the postulated flaw.

As stated earlier, the evaluations described above considering circumferentially oriented flaws cover longitudinal cases in pipes and elbows. The likelihood of a split in the elbows is very low because of the fact that the elbows are [$]^{a,c,e}$ and no flaws are actually anticipated. The prediction methods for failure in elbows are virtually the same as those for [

$]^{a,c,e}$

Therefore, the probability of any longitudinal flaw existing in the RHR line is much smaller when compared with the circumferential direction. Based on the above, it is judged that circumferential flaws are more limiting than longitudinal flaws in elbows and throughout the system.

Several computer codes are used in the evaluations. The main-frame computer programs are under Configuration Control which has requirements conforming to Standard Review Plan 3.9.1. The fracture mechanics calculations are independently verified. The computer codes used in this evaluation have been validated (bench marked) as described in references (1-5) and (1-6).

1.3 References

1-1 Report of the U.S. Nuclear Regulatory Commission Piping Review Committee - Evaluation of Potential for Pipe Breaks, NUREG 1061, Volume 3, November 1984.

1-2 Kumar, V., German, M. D. and Shih, C. P. "An Engineering Approach for Elastic-Plastic Fracture Analysis," EPRI Report NP-1931, Project 1237-1, Electric Power Research Institute, July 1981.

1-3 NUREG/CR-3464, 1983, "The Application of Fracture Proof Design Methods Using Tearing Instability Theory to Nuclear Piping Postulated Circumferential Through Wall Cracks."

1-4 Begley, J.A., et. al., "Crack Propagation Investigation Related to the Leak-Before-Break Concept for LMFBR Piping" in Proceedings, Conference on Elastic Plastic Fracture, Institution of Mechanical Engineers, London 1978.

1-5 Swamy, S. A., et al., "Additional Information in Support of the Elimination of Postulated Pipe Ruptures in the Pressurizer Surge Lines of South Texas Project Units 1 and 2" WCAP-11256, September 1986, Westinghouse Proprietary Class 2.

1-6 Swamy, S. A. et al., "Technical Basis for Eliminating Pressurizer Surge Line Ruptures as the Structural Design Basis for South Texas Project Units 1 and 2," WCAP-11256 Supplement 1, November 1986, Westinghouse Proprietary Class 2.

RCL HOT LEG

12" SCH 140

ISOLATION VALVE

Moderate Energy
Piping
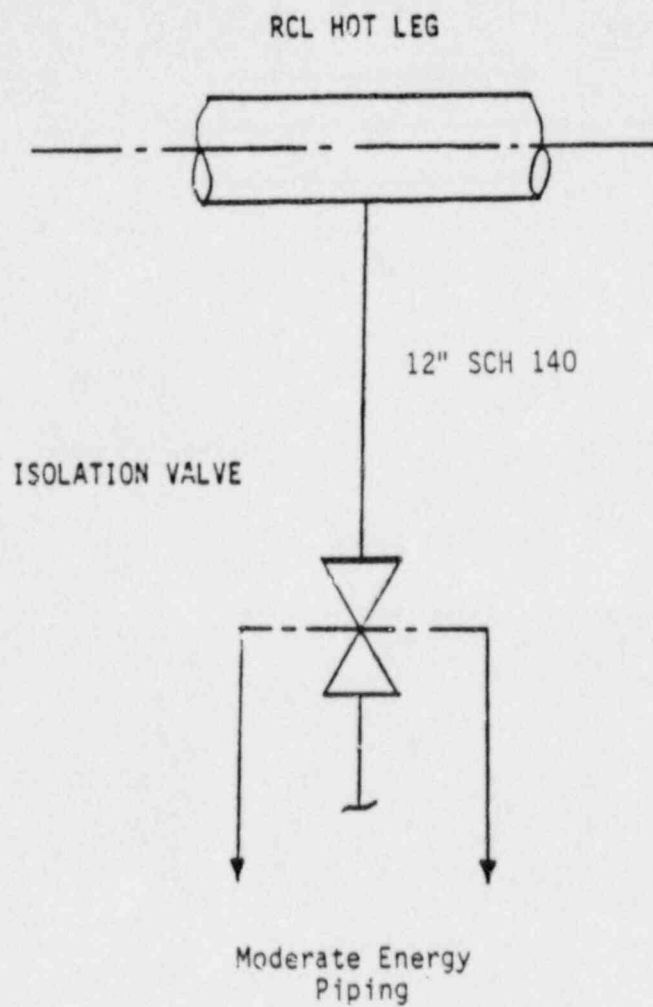
Figure 1-1 South Texas RHR Line Scope of Evaluation

SECTION 2.0

FAILURE CRITERIA FOR FLAWED PIPES

2.1 General Considerations

Active research is being carried out in industry and universities as well as
other research organizations to establish fracture criteria for ductile
materials. Criteria being investigated include those based on J-integral
initiation toughness, equivalent ene , crack opening displacement, crack
opening stretch, crack opening angle, net-section yield, tearing modulus and
void nucleation. Several of these criteria are discussed in an ASTM
publication (2-1).

A practical approach based on the ability to obtain material properties and to
make calculations using the available tools was used in selecting the criteria
for this investigation. The ultimate objective is to show that the RHR line
containing a conservatively assumed circumferential through-wall flaw is
stable under the worst combination of postulated faulted and operating
condition loads within acceptable engineering accuracy. With this viewpoint,
two mechanisms of failure, namely, local and global failure mechanisms are
considered.

2.2 Global Failure Mechanism

For a tough ductile material which is notch insensitive the global failure
will be governed by plastic collapse. Extensive literature is available on
this subject. A Pressure Vessel Research Committee study (2-2) reviews the
literature as well as data from several tests on piping components, and
discusses the details of analytical methods, assumptions and methods of
correlating experiments and analysis.

A schematic description of the plastic behavior and the definition of plastic
load is shown in Figure 2-1. For a given geometry and loading, the plastic
load is defined to be the peak load reached in a generalized load versus
displacement plot and corresponds to the point of instability.

A simplified version of this criterion, namely, net section yield criterion has been successfully used in the prediction of the load carrying capacity of pipes containing gross size through-wall flaws (2-3) and was found to correlate well with experiment. This criterion can be summarized by the following relationship:

$$Wa < Wp \qquad (2-1)$$

where Wa = applied generalized load
       Wp = calculated generalized plastic load

Wp represents the load carrying capacity of the cracked structure and it can be obtained by an elastic-plastic finite element analysis or by empirical correlation which is based on the material flow properties as discussed in Section 6.1

2.3 Local Failure Mechanism

The local mechanism of failure is primarily dominated by the crack tip behavior in terms of crack-tip blunting, initiation, extension and finally crack instability. The material properties and geometry of the pipe, flaw size, shape and loadings are parameters used in the evaluation of local failure.

The stability will be assumed if the crack does not initiate at all. It has been demonstrated that the initiation toughness, measured in terms of J_{Ic} from a J-integral resistance curve, is a material parameter defining the crack initiation. If, for a given load, the calculated J-integral value is shown to be less than J_{Ic} of the material, then the crack will not initiate.

If the initiation criterion is not met, one can calculate the tearing modulus as defined by the following relation:

$$T_{app} = \frac{dJ}{da} \frac{E}{\sigma_f^2} \qquad (2-2)$$

where T_{app} = applied tearing modulus

E = modulus of elasticity

σ_f = flow stress = $(\sigma_y + \sigma_u)/2$

a = crack length

σ_y, σ_u = yield and ultimate strength of the material respectively.

Stability then is said to exist when ductile tearing occurs if T_{app} is less than T_{mat}, the experimentally determined tearing modulus. Hence, the local crack stability is established by the two-step criteria:

$$J < J_{Ic}, \text{ or} \tag{2-3}$$

$$T_{app} < T_{mat}, \text{ if } J \geq J_{Ic} \tag{2-4}$$

2.4 References

2-1 J.D. Landes, et al., Editors, Elastic-Plastic Fracture, STP-668, ASTM, Philadelphia, PA 19109, November 1977.

2-2 J. C. Gerdeen, "A Critical Evaluation of Plastic Behavior Data and a Unified Definition of Plastic Loads for Pressure Components," Welding Research Council Bulletin No. 254.

2-3 Mechanical Fracture Predictions for Sensitized Stainless Steel Piping with Circumferential Cracks, EPRI-NP-192, September 1976.
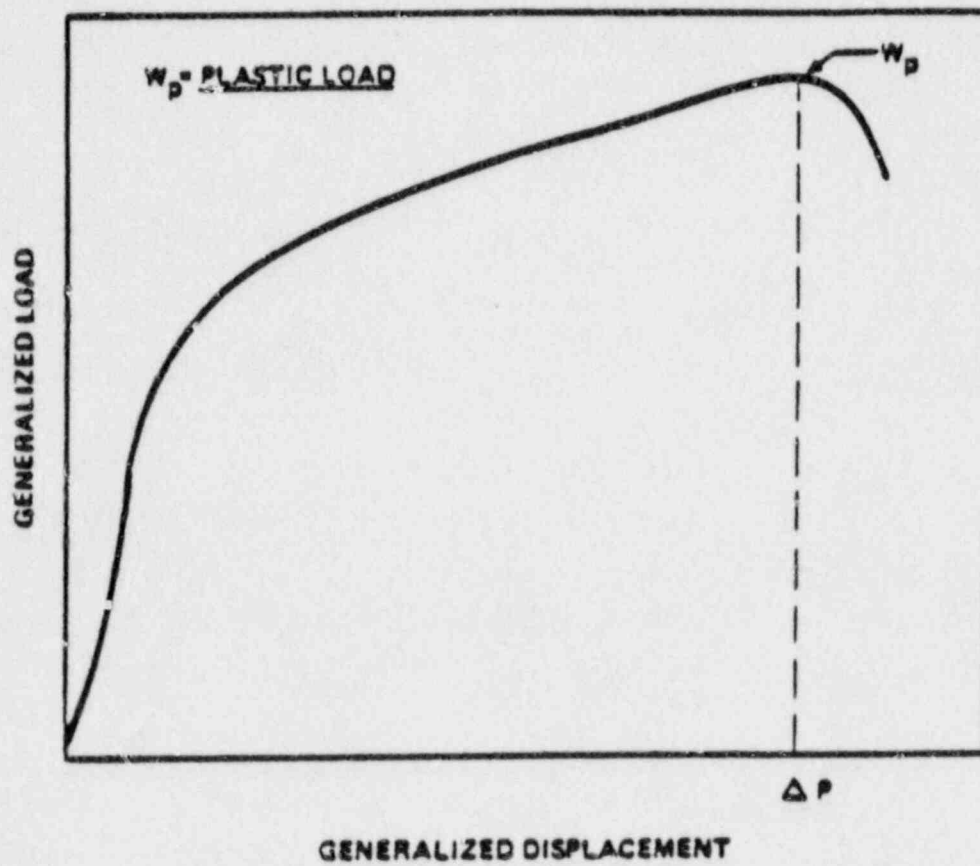
Figure 2-1 Schematic of Generalized Load-Deformation Behavior

2-4

SECTION 3.0

OPERATION AND STABILITY OF THE RHR LINE
AND THE REACTOR COOLANT SYSTEM

3.1 Stress Corrosion Cracking

The Westinghouse reactor coolant system primary loop and connecting Class 1
lines have an operating history that demonstrates the inherent stability
characteristics of the design. This includes a low susceptibility to cracking
failure from the effects of corrosion (e.g., intergranular stress corrosion
cracking). This operating history totals over 400 reactor-years, including
five plants each having over 17 years of operation and 15 other plants each
with over 12 years of operation.

In 1978, the United States Nuclear Regulatory Commission (USNRC) formed the
second Pipe Crack Study Group. (The first Pipe Crack Study Group established
in 1975 addressed cracking in boiling water reactors only.) One of the
objectives of the second Pipe Crack Study Group (PCSG) was to include a review
of the potential for stress corrosion cracking in Pressurized Water Reactors
(PWR's). The results of the study performed by the PCSG were presented in
NUREG-0531 (Reference 3-1) entitled "Investigation and Evaluation of Stress
Corrosion Cracking in Piping of Light Water Reactor Plants." In that report
the PCSG stated:

"The PCSG has determined that the potential for stress-corrosion cracking
in PWR primary system piping is extremely low because the ingredients
that produce IGSCC are not all present. The use of hydrazine additives
and a hydrogen overpressure limit the oxygen in the coolant to very low
levels. Other impurities that might cause stress-corrosion cracking,
such as halides or caustic, are also rigidly controlled. Only for brief
periods during reactor shutdown when the coolant is exposed to the air
and during the subsequent startup are conditions even marginally capable

of producing stress-corrosion cracking in the primary systems of PWRs. Operating experience in PWRs supports this determination. To date, no stress-corrosion cracking has been reported in the primary piping or safe ends of any PWR."

During 1979, several instances of cracking in PWR feedwater piping led to the establishment of the third PCSG. The investigations of the PCSG reported in NUREG-0691 (reference 3-2) further confirmed that no occurrences of IGSCC have been reported for PWR primary coolant systems.

As stated above, for the Westinghouse plants there is no history of stress corrosion cracking failure in the reactor coolant loop or connecting Class 1 piping. The discussion below further qualifies the PCSG's findings.

For stress corrosion cracking (SCC) to occur in piping, the following three conditions must exist simultaneously: high tensile stresses, susceptible material, and a corrosive environment. Since some residual stresses and some degree of material susceptibility exist in any stainless steel piping, the potential for stress corrosion is minimized by properly selecting a material immune to SCC as well as preventing the occurrence of a corrosive environment. The material specifications consider compatibility with the system's operating environment (both internal and external) as well as other material in the system, applicable ASME Code rules, fracture toughness, welding, fabrication, and processing.

The elements of a water environment known to increase the susceptibility of austenitic stainless steel to stress corrosion are: oxygen, fluorides, chlorides, hydroxides, hydrogen peroxide, and reduced forms of sulfur (e.g., sulfides, sulfites, and thionates). Strict pipe cleaning standards prior to operation and careful control of water chemistry during plant operation are used to prevent the occurrence of a corrosive environment. Prior to being put into service, the piping is cleaned internally and externally. During flushes and preoperational testing, water chemistry is controlled in accordance with written specifications. Requirements on chlorides, fluorides, conductivity, and pH are included in the acceptance criteria for the piping.

3-2

During plant operation, the reactor coolant water chemistry is monitored and maintained within very specific limits. Contaminant concentrations are kept below the thresholds known to be conducive to stress corrosion cracking with the major water chemistry control standards being included in the plant operating procedures as a condition for plant operation. For example, during normal power operation, oxygen concentration in the RCS and connecting Class 1 lines is expected to be in the ppb range by controlling charging flow chemistry and maintaining hydrogen in the reactor coolant at specified concentrations. Halogen concentrations are also stringently controlled by maintaining concentrations of chlorides and fluorides within the specified limits. Thus during plant operation, the likelihood of stress corrosion cracking is minimized.

3.2 Water Hammer

Overall, there is a low potential for water hammer in the RCS and connecting RHR lines since they are designed and operated to preclude the voiding condition in normally filled lines. The RCS and connecting RHR lines including piping and components, are designed for normal, upset, emergency, and faulted condition transients. The design requirements are conservative relative to both the number of transients and their severity. Relief valve actuation and the associated hydraulic transients following valve opening are considered in the system design. Other valve and pump actuations are relatively slow transients with no significant effect on the system dynamic loads. To ensure dynamic system stability, reactor coolant parameters are stringently controlled. Temperature during normal operation is maintained within a narrow range by control rod position; pressure is controlled by pressurizer heaters and pressurizer spray also within a narrow range for steady-state conditions. The flow characteristics of the system remain constant during a fuel cycle because the only governing parameters, namely system resistance and the reactor coolant pump characteristics are controlled in the design process. Additionally, Westinghouse has instrumented typical reactor coolant systems to verify the flow and vibration characteristics of the system and connecting RHR lines. Preoperational testing and operating

experience have verified the Westinghouse approach. The operating transients of the RCS primary piping and connected RHR lines are such that no significant water hammer can occur.

3.3 Low Cycle and High Cycle Fatigue

Low cycle fatigue considerations are accounted for in the design of the piping system through the fatigue usage factor evaluation to show compliance with the rules of Section III of the ASME Code. A further evaluation of the low cycle fatigue loading is discussed in Chapter 7 and Appendix B as part of this study in the form of a fatigue crack growth analysis.

High cycle fatigue loads in the system would result primarily from pump vibrations during operation. During operation, an alarm signals the exceedance of the RC pump shaft vibration limits. Field measurements have been made on the reactor coolant loop piping of a number of plants during hot functional testing. Stresses in the elbow below the RC pump have been found to be very small, between 2 and 3 ksi at the highest. When translated to the connecting RHR lines, these stresses are even lower, well below the fatigue endurance limit for the RHR line material and would result in an applied stress intensity factor below the threshold for fatigue crack growth.

3.4 Potential Degradation During Service

In the Westinghouse PWR design there has never been any service cracking identified in the RHR piping. Only one incident of wall thinning has been identified in RHR lines of Westinghouse PWR design. However, this is of no concern in the present application as described later in this section. Sources of such degradation are mitigated by the design, construction, inspection, and operation of the RHR lines.

Based on a review of references 3-3 through 3-6 only one incident of water hammer has been reported in a PWR RHR system. This incident was a result of incorrect valve line-up preceding a pump start. The only damage sustained was

to several pipe supports. Therefore it is concluded that water hammer in the RHR system is unlikely to affect piping integrity or to cause pipe system degradation.

Wall thinning by erosion and erosion-corrosion effects will not occur in the RHR line due to the low velocity, typically less than 10 ft/sec and the material, austenitic stainless steel, which is highly resistant to these degradation mechanisms. Per NUREG-0691 [3-2], a study of " :e cracking in PWR piping, only two incidents of wall thinning in stainless steel pipe were reported. One incident was related to the RHR system. However, this occurred in the pump recirculation path which has higher flow velocity and is more susceptible to other contributing factors such as cavitation, than the RHR piping near the primary loop. Therefore, wall thinning is not a significant concern in the portion of the system being addressed in this evaluation.

Flow stratification, where low flow conditions permit cold and hot water to separate into distinct layers, can cause significant thermal fatigue loadings. This was an important issue in PWR feedwater piping where temperature differences of 300°F were not uncommon under certain operational conditions. Stratification is believed to be important where low flow conditions and a temperature differential exist. This is not an issue in the RHR line, where typically there is no flow during normal plant operation. During RHR operation the flow causes sufficient mixing to eliminate stratification.

On December 9, 1987, while Alabama Power and Light Company's Farley Nuclea, Power Station Unit 2 was at 33% power (during a restart following a refueling cutage) a total unidentified RCS leak of 0.7 gpm was detected [3-7]. The source of the leak was identified as a through-wall crack in a weld joint between an elbow and a horizontal pipe section in the 6 inch safety injection (SI) line attached to the cold leg of reactor coolant loop B. In order to identify the mechanism which caused the crack, instrumentation was placed on the replaced piping and on a reference line to monitor temperatures and accelerations during heatup and operation. The results of this study indicated the existence of thermal cycling and stratification in the vicinity

of the cracked weld. The observed thermal cycling and stratification, due to the leakage past the single isolation valve between the charging system and the safety injection system, have been postulated to have caused the through-wall crack of the 6 inch SI line. This is the first such reported instance of this mechanism resulting in a through-wall crack on Class 1 pipe. At South Texas Projects Units 1 and 2, the RHR system configuration does not include a potential leakage path. Therefore, thermal stratification is not expected to occur in the horizontal sections of the RHR lines.

The maximum normal operating temperature of the RHR piping is about 623°F. This is well below the temperature which would cause any creep damage in stainless steel piping.

3.5 Assessment of Pipe Degradation or Failure from Indirect Causes

Pipe degradation or failure from indirect causes such as fires, missiles, and component support failure is prevented by designing, fabricating, and inspecting reactor compartments, components, and supports, to NRC criteria that reduce to a low probability the likelihood of the events unacceptably impacting safety related components. South Texas Project complies with the criteria in Standard Review Plans 3.4.1, 3.5.1.2, 3.9.3, 3.9.6, and 9.5.1 as discussed in these same sections in the FSAR.

It can be concluded by review of these sections of the South Texas FSAR that the required measures are taken to preclude the degradation or failure from outside sources of piping in the plant and that the methods utilized are consistent with those given in the Standard Review Plan.

3.6 References

3-1 Investigation and Evaluation of Stress-Corrosion Cracking in Piping of Light Water Reactor Plants, NUREG-0531, U.S. Nuclear Regulatory Commission, February 1979.

3-2 Investigation and Evaluation of Cracking Incidents in Piping in Pressurized Water Reactors, NUREG-0691, U.S. Nuclear Regulatory Commission, September 1980.

3-3 Utter, R. A., et. al., "Evaluation of Water Hammer Events in Light Water Reactor Plants," NUREG/CR-2781, published July 1982.

3-4 "Report of the U.S. Nuclear Regulatory Commission Piping Review Committee, Evaluation of Other Dynamic Loads and Load Combinations," NUREG-1061 Volume 4, Published December 1984.

3-5 Chapman, R. L., et. al., "Compilation of Data Concerning Known and Suspected Water Hammer Events in Nuclear Power Plants, CY 1969-May 1981," NUREG/CR-2059, Published April 1982.

3-6 "Evaluation of Water Hammer Occurrence in Nuclear Power Plants," NUREG-0929 Revision 1, Published March 1984.

3-7 NRC Bulletin No. 88-08, Thermal Stresses in Piping Connected to Reactor Coolant Systems, Nuclear Regulatory Commission, June 22, 1988.

SECTION 4.0

MATERIAL CHARACTERIZATION

4.1 Pipe, Fittings and Weld Materials

The pipe material of the RHR line is SA376-TP316, a wrought product form of
the type used for the primary loop piping of several PWR plants. The RHR line
is connected to the primary loop nozzle. The other end of the RHR line is
connected to an isolation valve. The piping layout includes fittings such as
elbows. These elbows are SA403-WP316 steel which is wrought and formed pipe
of SA182-TP316 material. The weld wire used in the shop fabrication is
generally of low carbon 316L. The field weld used 308L weld wire. The
welding processes used are gas tungsten arc (GTAW), submerged arc (SAW) and
shielded metal arc (SMAW).

In the following sections the tensile and fracture toughness properties of
these materials are presented and criteria for use in the leak-before-break
analyses are defined.

4.2 Tensile Properties

The material certifications provided by reference 4-5 for the RHR lines of the
Units 1 and 2 were used to establish the tensile properties for the piping,
fittings and welds. These properties are given in tables 4-1 through 4-6.
The properties in these tables are at room temperature. In the leak-before-
break evaluation presented in this report, the minimum properties at operating
temperature (623°F) are used for the flaw stability evaluation and average
properties are used for the leak rate predictions. The viability of using
such properties for the RHR line is presented below.

As noted in tables 4-1 through 4-6, the specific room temperature properties
of the RHR line heats compare favorably with the properties of similar
material of the primary loops (see table 4-7). [

]^{a,c,e}

4-1

[

]a,c,e

In brief, the following material properties were used in the analyses set forth in this report.

Minimum Properties for Flaw Stability Analysis (623°F)

[   ] a,c,e

Average Properties for Leak Rate Calculations (623°F)

[   ] a,c,e

4.3 Fracture Toughness Properties

Series of fracture toughness tests on SA376-TP316 pipe material and E308 welds are reported in references 4-2 and 4-3. Data from these tests at 600°F are summarized in table 4-8. As seen from this table, the lowest J_{Ic} value for the weld materials observed from the J-R curves was [ ]^{a,c,e} in-lb/in^2. The T_{mat} corresponding to this value of J_{Ic} was over [ ]^{a,c,e}. The sample yielding the lowest slope of the J-R curve had a T_{mat} of [ ]^{a,c,e}. The corresponding J_{Ic} was found to be around [ ]^{a,c,e} in-lb/in^2. While the data on welds cited above show superior toughness properties, they were not used in the leak-before-break evaluation. Instead, lower bound toughness data for the SMAW welds (noting that the weld at the governing location was GTAW) were used as follows:

The data on SMAW welds based on testing 1T specimens presented in reference 4-4 can be considered as lower bound toughness data. The resulting test data are as follows:

$$J_{Ic} = 959 \text{ in-lb/in}^2$$

$$J_{max} \simeq 3000 \text{ in-lb/in}^2$$

$$T_{mat} = 140 \text{ (corresponding to } J_{max})$$

The J versus T for the data is plotted in figure 4-3.

The nozzles connecting the RHR Lines with the primary loop are made of forged stainless steel. Forged stainless steel is considered not susceptible to thermal aging for applications at hand.

4.4 References

4-1 Nuclear Systems Materials Handbook, Part I - Structural Materials, Group 1 - High Alloy Steels, Section 4, ERDA Report TID 26666, November 1975 Revision.

4-2 S. S. Palusamy, "Tensile and Toughness Properties of Primary Piping Weld Metal for Use in Mechanistic Fracture Evaluation," WCAP 9787, May, 1981 (Westinghouse Proprietary Class 2).

4-3 S. S. Palusamy, et al., "Mechanistic Fracture Evaluation of Reactor Coolant Pipe Containing a Postulated Circumferential Through-Wall Crack," WCAP-9558, Rev. 2, May 1982, (Westinghouse Proprietary Class 2).

4-4 Toughness of Austenitic Stainless Steel Pipe Welds, EPRI-NP-4768, Electric Power Research Institute, October 1986.

4-5 Project letter ST-YB-WN-1921, from A. Matiuk (Bechtel Energy Corporation) to J. W. Irons (Westinghouse Electric Corporation), dated December 16, 1987.

TABLE 4-1

MATERIAL PROPERTIES OF STP UNIT-1, LOOP 1 RHR LINE
AT 70°F AS DETERMINED BY TESTING

PRODUCT	HEAT NO.	MATERIAL	ULTIMATE STRENGTH (PSI)	.2% OFFSET YIELD STRESS (PSI)	% ELONG PER INCH	% RED IN AREA
Elbow	55894	SA403(182)/WP316	79,000	50,500	45.00	70.50
Elbow	53897	SA403(182)/WP316	81,500	48,500	56.50	74.50
Elbow	53897	SA403(182)/WP316	81,500	48,500	56.50	74.50
Pipe	L5093	SA376/TP316	88,200	42,700	53.20	64.10
Pipe	L5093	SA376/TP316	88,200	42,700	53.20	64.10
Pipe	L5093	SA376/TP316	88,200	42.700	53.20	64.10
Weld	17138	SFA5.9-ER316L	88,700	65,400	48.00	65.90
Weld	17138	SFA5.9-ER316L	83,600	67,200	50.00	65.50
Weld	17138	SFA5.9-ER316L	83,600	67,200	50.00	65.50
Weld	17138	SFA5.9-ER316L	88,700	65,400	48.00	65.90
Weld	17138	SFA5.9-ER316L	83,600	67,200	50.00	65.50
Weld	17138	SFA5.9-ER316L	88,700	65,400	48.00	65.90
Weld	17138	SFA5.9-ER316L	83,600	67,200	50.00	65.50
Weld	17138	SFA5.9-ER316L	88,700	65,400	48.00	65.90
Weld	17138	SFA5.9-ER316L	83,600	67,200	50.00	65.50
Pipe	L5093	SA376/TP316	88,700	42,700	53.20	64.10
Weld	17138	SFA5.9-ER316L	83,600	67,200	50.00	65.50
Elbow	55894	SA403(182)/WP316	79,000	50,500	45.00	70.50
Pipe	P8608	SA376-TP316	85,600	43,300	58.50	71.70
Pipe	P8608	SA376-TP316	85,600	43,300	58.50	71.70
Weld	17138	SFA5.9-ER316L	83,600	67,200	50.00	65.50
Weld	17138	SFA5.9-ER316L	83,600	67,200	50.00	65.50
Weld	17138	SFA5.9-ER316L	88,700	65,400	48.00	65.90
Weld	17138	SFA5.9-ER316L	83,600	67,200	50.00	65.50
Weld	17138	SFA5.9-ER316L	83,600	67,200	50.00	65.50

TABLE 4-2

MATERIAL PROPERTIES OF STP UNIT-1, LOOP 2 RHR LINE
AT 70°F AS DETERMINED BY TESTING

PRODUCT	HEAT NO.	MATERIAL	ULTIMATE STRENGTH (PSI)	.2% OFFSET YIELD STRESS (PSI)	% ELONG PER INCH	% RED IN AREA
Elbow	55895	SA403(182)/WP316	81,500	51,000	56.00	74.50
Elbow	53897	SA403(182)/WP316	81,500	48,500	56.50	74.50
Elbow	53897	SA403(182)/WP316	81,500	48,500	56.50	74.50
Pipe	L5093	SA376/TP316	81,400	44,500	61.00	77.30
Pipe	L5093	SA376/TP316	81,400	44,500	61.00	77.30
Pipe	L5093	SA376/TP316	81,400	44,500	61.00	77.30
Weld	17138	SFA5.9-ER316L	86,700	62,600	36.00	65.40
Weld	17138	SFA5.9-ER316L	83,600	67,200	50.00	65.50
Weld	17138	SFA5.9-ER316L	86,700	62,600	36.00	65.40
Weld	17138	SFA5.9-ER316L	83,600	67,200	50.00	65.50
Weld	0575	SFA5.4/E316L	80,400	57,400	45.00	63.80
Weld	17138	SFA5.9/ER316L	83,600	67,200	50.00	65.50
Weld	17138	SFA5.9/ER316L	86,700	62,600	36.00	65.40
Weld	17138	SFA5.9/ER316L	83,600	67,200	50.00	65.50
Weld	17138	SFA5.9/ER316L	86,700	62,600	36.00	65.40
Weld	17138	SFA5.9/ER316L	83,600	67,200	50.00	65.50
Pipe	P8607	SA376/TP316	89,800	43,900	53.00	71.70

TABLE 4-3

MATERIAL PROPERTIES OF STP UNIT-1, LOOP 3 RHR LINE
AT 70°F AS DETERMINED BY TESTING

PRODUCT	HEAT NO.	MATERIAL	ULTIMATE STRENGTH (PSI)	.2% OFFSET YIELD STRESS (PSI)	% ELONG PER INCH	% RED IN AREA
Elbow	55895	SA403(182)/WP316	81,500	51,000	56.00	74.50
Elbow	53897	SA403(182)/WP316	81,500	48,500	56.50	74.50
Elbow	53897	SA403(182)/WP316	81,500	48,500	56.50	74.50
Pipe	L5093	SA376/TP316	81,400	44,500	61.00	77.30
Pipe	L5093	SA376/TP316	81,400	44,500	61.00	77.30
Pipe	L5093	SA376/TP316	81,400	44,500	61.00	77.30
Pipe	L5093	SA376/TP316	81,400	44,500	61.00	77.30
Weld	0575	SFA5.4/E316L	80,400	57,400	45.00	63.80
Weld	17138	SFA5.9/ER316L	83,600	67,200	30.00	65.50
Weld	17138	SFA5.9/ER316L	86,700	62,600	36.00	65.40
Weld	17138	SFA5.9/ER316L	83,600	67,200	50.00	65.50
Weld	17138	SFA5.9/ER316L	86,700	62,600	36.00	65.40
Weld	17138	SFA5.9/ER316L	83,600	67,200	50.00	65.50
Weld	0683A	SFA5.4/E316L	79,700	58,600	40.00	66.20
Weld	0575	SFA5.4/E316L	80,400	57,400	45.00	63.80
Weld	17138	SFA5.9/ER316L	83,600	67,200	50.00	65.50
Weld	17138	SFA5.9/ER316L	86,700	62,600	36.00	65.40
Weld	17138	SFA5.9/ER316L	83,600	67,200	50.00	65.50
Weld	17138	SFA5.9/ER316L	86,700	62,600	36.00	65.40
Weld	17138	SFA5.9/ER316L	83,600	67,200	50.00	65.50
Pipe	P8607	SA376/TP316	89,800	43,900	53.00	71.70
Elbow	55894	SA403(182)/WP316	79,000	50,500	45.00	70.50
Pipe	L5093	SA376/TP316	81,400	44,500	61.00	77.30
Weld	17138	SFA5.9-ER316L	86,700	62,600	36.00	65.40
Weld	17138	SFA5.9-ER316L	83,600	67,200	50.00	65.50

4-7

TABLE 4-4

MATERIAL PROPERTIES OF STP UNIT-2, LOOP 1 RHR LINE
AT 70°F AS DETERMINED BY TESTING

PRODUCT	HEAT NO.	MATERIAL	ULTIMATE STRENGTH (PSI)	.2% OFFSET YIELD STRESS (PSI)	% ELONG PER INCH	% RED IN AREA
Elbow	55894	SA403(182)/WP316	79,000	50,500	45.00	70.50
Elbow	53897	SA403(182)/WP316	81,500	48,500	56.50	74.50
Elbow	43897	SA403(182)/WP316	81,500	48,500	56.50	74.50
Pipe	L5091	SA376-TP316	82,600	38,100*	60.50	71.20
Pipe	P8607	SA376-TP316	89,800	43,900	53.00	71.70
Pipe	L5091	SA376-TP316	88,600	44,100	52.00	67.30
Weld	17138	SFA5.9/ER316L	86,700	62,600	36.00	65.40
Weld	17138	SFA5.9/ER316L	83,600	67,200	50.00	65.50
Weld	17138	SFA5.9/ER316L	83,600	67,200	50.00	65.50
Weld	17138	SFA5.9/ER316L	86,700	62,600	36.00	65.40
Weld	0575	SFA5.4E316L	80,400	57,400	45.00	63.80
Weld	17138	SFA5.9/ER316L	83,600	67,200	50.00	65.50
Weld	17138	SFA5.9/ER316L	83,600	67,200	50.00	65.50
Weld	17138	SFA5.9/ER316L	86,700	62,600	36.00	65.40
Weld	17138	SFA5.9/ER316L	83,600	67,200	50.00	65.50
Weld	17138	SFA5.9/ER316L	86,700	62,600	36.00	65.40
Pipe	L5091	SA376/TP316	87,800	43,300	56.00	66.00
Weld	17138	SFA5.9-ER316L	83,600	67,200	50.00	65.50
Elbow	55893	SA403(182)/WP316	81,500	49,000	62.00	75.50
Pipe	P8607	A376/TP316	89,800	43,900	53.00	71.70
Pipe	L5091	SA376/TP316	87,800	43,300	56.00	66.00
Weld	0575	SFA5.4/E316L	80,400	57,400	45.00	63.80
Weld	17138	SFA5.9/ER316L	83,600	67,200	50.00	65.50
Weld	17138	SFA5.9/ER316L	86,700	62,600	36.00	65.40
Weld	17138	SFA5.9/ER316L	83,600	67,200	50.00	65.50

*The lowest room temperature yield stress

TABLE 4-5

MATERIAL PROPERTIES OF STP UNIT-2, LOOP 2 RHR LINE
AT 70°F AS DETERMINED BY TESTING

PRODUCT	HEAT NO.	MATERIAL	ULTIMATE STRENGTH (PSI)	.2% OFFSET YIELD STRESS (PSI)	% ELONG PER INCH	% RED IN AREA
Elbow	55895	SA403(182)/WP316	81,500	51,000	56.00	74.50
Elbow	53897	SA403(182)/WP316	81,500	48,500	56.50	74.50
Elbow	53897	SA403(182)/WP316	81,500	48,500	56.50	74.50
Pipe	L5093	SA376/TP316	81,400	44,500	61.00	77.30
Pipe	L5093	SA376/TP316	81,400	44,500	61.00	77.30
Pipe	L5093	SA376/TP316	84,600	40,500	59.50	68.20
Weld	17138	SFA5.9-ER316L	86,700	62,600	36.00	65.40
Weld	17138	SFA5.9-ER316L	83,600	67,200	50.00	65.50
Weld	17138	SFA5.9-ER316L	83,600	67,200	50.00	65.50
Weld	17138	SFA5.9-ER316L	86,700	62,600	36.00	65.40
Weld	0575	SFA5.4/E316L	80,400	57,400	45.00	63.80
Weld	17138	SFA5.9/ER316L	83,600	67,200	50.00	65.50
Weld	17138	SFA5.9/ER316L	83,600	67,200	50.00	65.50
Weld	17138	SFA5.9/ER316L	86,700	62,600	36.00	65.40
Weld	17138	SFA5.9/ER316L	83,600	67,200	50.00	65.50
Weld	17138	SFA5.9/ER316L	86,700	62,600	36.00	65.40
Pipe	P8607	SA376/TP316	89,800	43,800	53.00	71.70

TABLE 4-6

MATERIAL PROPERTIES OF STP UNIT-2, LOOP 3 RHR LINE
AT 70°F AS DETERMINED BY TESTING

PRODUCT	HEAT NO.	MATERIAL	ULTIMATE STRENGTH (PSI)	.2% OFFSET YIELD STRESS (PSI)	% ELONG PER INCH	% RED IN AREA
Elbow	53894	SA403(182)/WP316	77,500	43,000	65.00	76,50
Elbow	53897	SA403(182)/WP316	81,500	48,500	56.50	74.50
Elbow	53897	SA403(182)/WP316	81,500	48,500	56.50	74.50
Pipe	L5093	SA376/TP316	81,400	44,500	61.00	77.30
Pipe	L5093	SA376/TP316	81,400	44,500	61.00	77.30
Pipe	L5093	SA376/TP316	81,400	44,500	61.00	77.30
Pipe	L5093	SA376/TP316	81,400	44,500	61.00	77.30
Weld	17138	SFA5.9/ER316L	83,600	67,200	50.00	65.50
Weld	0683A	SFA5.4/E316L	79,700	58,600	40.00	66.20
Weld	17138	SFA5.9/ER316L	86,700	62,600	36.00	65.40
Weld	17138	SFA5.9/ER316l.	83,600	67,200	50.00	65.50
Weld	17138	SFA5.9/ER316L	86,700	62,600	36.00	65.40
Weld	17138	SFA5.9/ER316L	83,600	67,200	50.00	65.50
Weld	0575	SFA5.4/E316L	80,400	57,400	45.00	63.80
Weld	0683A	SFA5.4/E316L	79,700	58,600	40.00	66.20
Weld	17138	SFA5.9/ER316L	83,600	67,200	50.00	65.50
Weld	17138	SFA5.9/ER316L	86,700	62,600	36.00	65.40
Weld	17138	SFA5.9/ER316L	83,600	67,200	50.00	65.50
Weld	17138	SFA5.9/ER316L	86,700	62,600	36.00	65.40
Weld	17138	SFA5.9/ER316L	83,600	67,200	50.00	65.50
Pipe	L5091	SA376/TP3167	87,800	43,300	56.00	66.00
Elbow	55894	SA403(182)/WP316	81,500	49,000	62.00	75.50
Pipe	L5093	SA376/TP316	81,400	44,500	61.00	77.30
Weld	17138	SFA5.9-ER316L	86,700	62.600	36.00	65.40
Weld	17138	SFA5.9-ER316L	83,600	67,200	50.00	65.50

TABLE 4-7

TYPICAL TENSILE PROPERTIES OF SA376 TP316, SA351 CF8A and WELDS OF SUCH MATERIAL FOR THE PRIMARY LOOP

Plant	Material	Test Temperature (°F)	Average Tensile Properties	
			Yield (psi)	Ultimate (psi)
A	SA376 TP316	70	40,900 (48)[a]	83,200 (48)
		650	23,500 (19)	67,900 (19)
	E 308 Weld	70	63,900 (3)	87,600 (3)
B	SA376 TP316	70	47,100 (40)	88,300 (40)
		650	26,900 (22)	69,100 (25)
	E 308 Weld	70	59,600 (8)	87,200 (8)
		650	31,500 (1)	68,800 (1)
C	SA376 TP316	70	46,600 (36)	87,300 (36)
		650	24,200 (18)	66,800 (19)
	E 308 Weld	70	61,900 (4)	85,400 (4)
D	SA351 CF8A	70	47,300 (14)	84,500 (14)
		650	26,000 (4)	70,500 (4)
	Weld	70	61,200 (31)	84,500 (32)

---

a. (____) indicates the number of test results averaged.

TABLE 4-8

FRACTURE TOUGHNESS PROPERTIES TYPICAL OF THE RHR LINE

Material	Test Temp. (°F)	Tensile Properties (psi) Yield	Ultimate	J_{Ic} (in-lb/in^2)	T_{mat}
SA376 TP316	600	21,700	65,500		
SA376 TP316	600	20,500	60,100		
Weld$_f$(E308 and E316)	600	45,000[b]	61,200[b]		
Weld$_f$	600	--	--		
SA351 CF8A[h]	600	--	--		

The J_{Ic} and T_{mat} columns are bracketed with the label a,c,e.

_____

[ ]a,c,e

  b. Lowest of 6 tests.

a,c,e

］a,c,e

Figure 4-1.   True Stress-True Strain Curve for SA376 TP 316 Stainless Steel
at 623°F (minimum properties)

a,c,e

Figure 4-2   True Stress-True Strain Curve for SA 376 TP 316 Stainless Steel
(Average Properties)
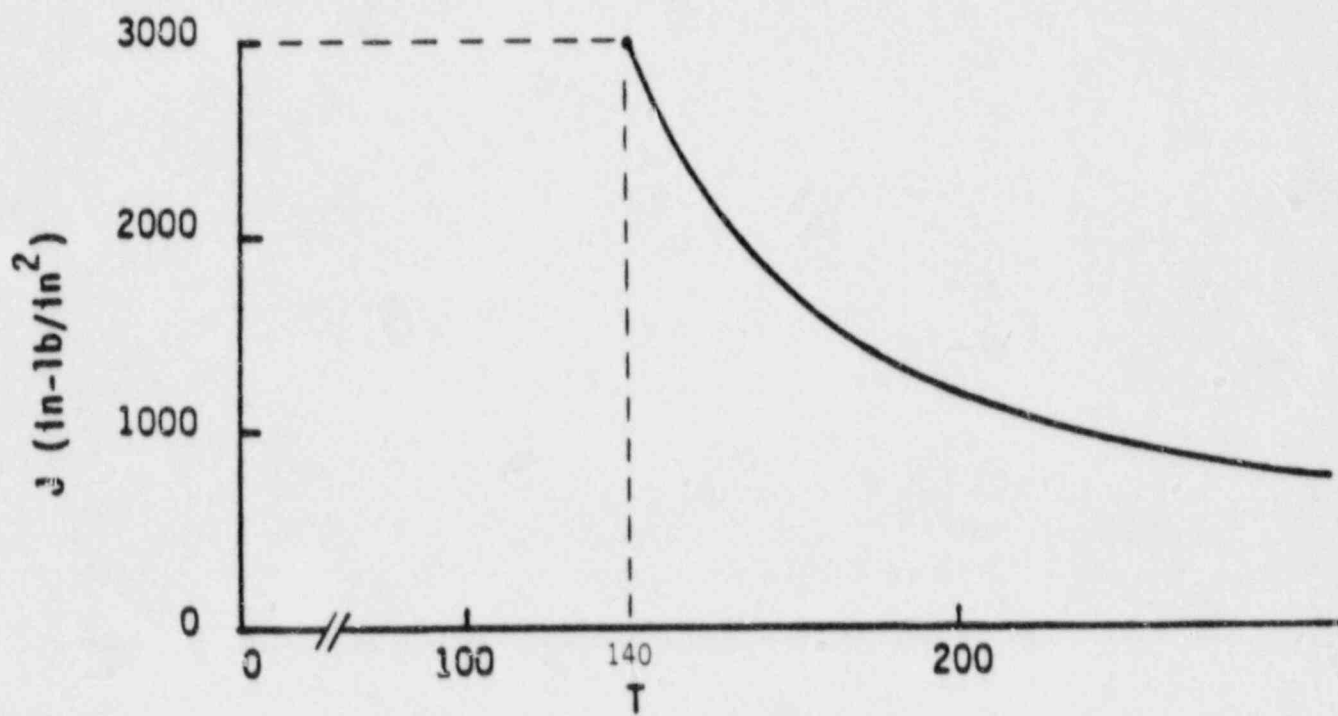
Figure 4-3. J versus T Curve for SMAW Welds

SECTION 5.0

LOADS FOR FRACTURE MECHANICS ANALYSIS

Figures 5-1 through 5-3 are schematic layouts of the RHR lines attached to the reactor coolant loops 1, 2, and 3 of South Texas Units 1 and 2. Highest and next highest stressed node locations are shown by the layout in figure 5-2.

The stresses due to axial loads and bending moments were calculated by the following equation:

$$\sigma = \frac{F}{A} + \frac{M}{Z} \tag{5.1}$$

where,

σ	=	stress
F	=	axial load
M	=	bending moment
A	=	metal cross-sectional area
Z	=	section modulus

The bending moments for the desired loading combinations were calculated by the following equation:

$$M = \sqrt{M_Y^2 + M_Z^2} \tag{5.2}$$

where,

M	=	bending moment for required loading
M_Y	=	Y component of bending moment
M_Z	=	Z component of bending moment

The axial load and bending moments for crack stability analysis and leak rate predictions were computed by the methods to be explained in Sections 5.1 and 5.2.

5.1 Loads for Crack Stability Analysis

The faulted loads for the crack stability analysis were calculated by the following equations:

$$F = |F_{DW} + F_{TH} + F_P| + |F_{SSE}| \tag{5.3}$$

$$M_Y = |(M_Y)_{DW} + (M_Y)_{TH}| + |(M_Y)_{SSE}| \tag{5.4}$$

$$M_Z = |(M_Z)_{DW} + (M_Z)_{TH}| + |(M_Z)_{SSE}| \tag{5.5}$$

Where, the subscripts of the above equations . . . snt the following loading cases,

DW = deadweight

TH = normal thermal expansion

SSE = SSE loading including seismic ancho; mo . .

P = load due to internal pressure

5.2 Loads for Leak Rate Evaluation

The normal operating loads for leak rate predictions were calculated by the following equations:

$$F = F_{DW} + F_{TH} + F_P \tag{5.6}$$

$$M_Y = (M_Y)_{DW} + (M_Y)_{TH} \tag{5.7}$$

$$M_Z = (M_Z)_{CW} + (M_Z)_{TH} \tag{5.8}$$

5.3 Summary of Loads, Geometry and Materials

Table 5-1 provides a summary of envelope loads computed for fracture mechanics evaluations in accordance with the methods described in section 5.1, and 5.2 (references 5-1 and 5-2). The cross-sectional dimensions and materials are also summarized. Load data are tabulated at the highest stressed location (node 135, loop 2), and the second highest stressed location (node 130E, loop 2). The loading components are provided in table 5-2.

All loads used in the LBB evaluation are for the as-built configuration. Unit 1 and Unit 2 have the same as-built normal loads at the governing location but the as-built normal plus SSE loads are slightly higher for Unit 2. The Unit 2 loads are used in the stability evaluations discussed in Section 6.0.

5.4 Governing Location

The normal plus SSE axial stresses along the RHR line starting from the primary loop nozzle junction up to the first isolation valve were compared. The maximum stress occurs at node 135 on the loop 2 RHR line. The welding process at this location is GTAW. This location is identified in figure 5-2. Detailed fracture mechanics analyses were performed at this highest stressed location.

5.5 References

5-1 Project Letter ST-YB-WN-1921, from A. Matiuk (Bechtel Energy Corporation) to J.W. Irons (Westinghouse Electric Corporation) dated December 16, 1987.

5-2 Project Letter ST-YB-WN-1937, from A. Matiuk (Bechtel Energy Corporation) to J. W. Irons (Westinghouse Electric Corporation) dated April 19, 1988.

TABLE 5-1

SUMMARY OF ENVELOPE LOADS

LOCATION	CONDITION	NODE NO	LOOP	MATERIAL	OUTSIDE DIA (inches)	SCHEDULE	NOMINAL WALL THICK (inches)	MINIMUM WALL THICK (inches)	INSIDE[a] DIA (inches)	F[b] (kips)	M[b] (in-kips)
Highest Load Location	Faulted	135	2	SA376 -TP3166	12.75	140	1.125	1.005	10.74	198	862
	Normal Operating	135	2	SA376 -TP316	12.75	140	1.125	1.005	10.74	196	395
Next Highest Load Location	Faulted	130E	2	SA376 -TP316	12.75	140	1.125	1.005	10.74	198	793
	Normal Operating	130E	2	SA376 -TP316	12.75	140	1.125	1.005	10.74	196	396

[a]Based on minimum wall thickness of 1.005 in.
[b]The stress based on the loads is 13.9 ksi using the minimum wall thickness.

5-4

TABLE 5-2

LOADING COMPONENTS AT GOVERNING LOCATIONS

Load Type	Highest Load (Location - 135, Loop 2)			Next Highest Load (Location - 130E, Loop 2)		
	Axial Force (lbs)	Bending Moment MY (ft-lb)	Bending Moment MZ (ft-lb)	Axial Force (lb)	Bending Moment MY (ft-lb)	Bending Moment MZ (ft-lb)
Dead Weight	-746	626	1027	-646	580	527
Thermal	1950	30,156	-12,683	1,948	30,351	-12,114
Pressure	194,828	-	-	194,828	-	-
SSE + Anch. Mot.	1792	36,808	12,691	1793	31,378	10,476

Hot Leg
Loop 1

Moderate
Energy
Piping
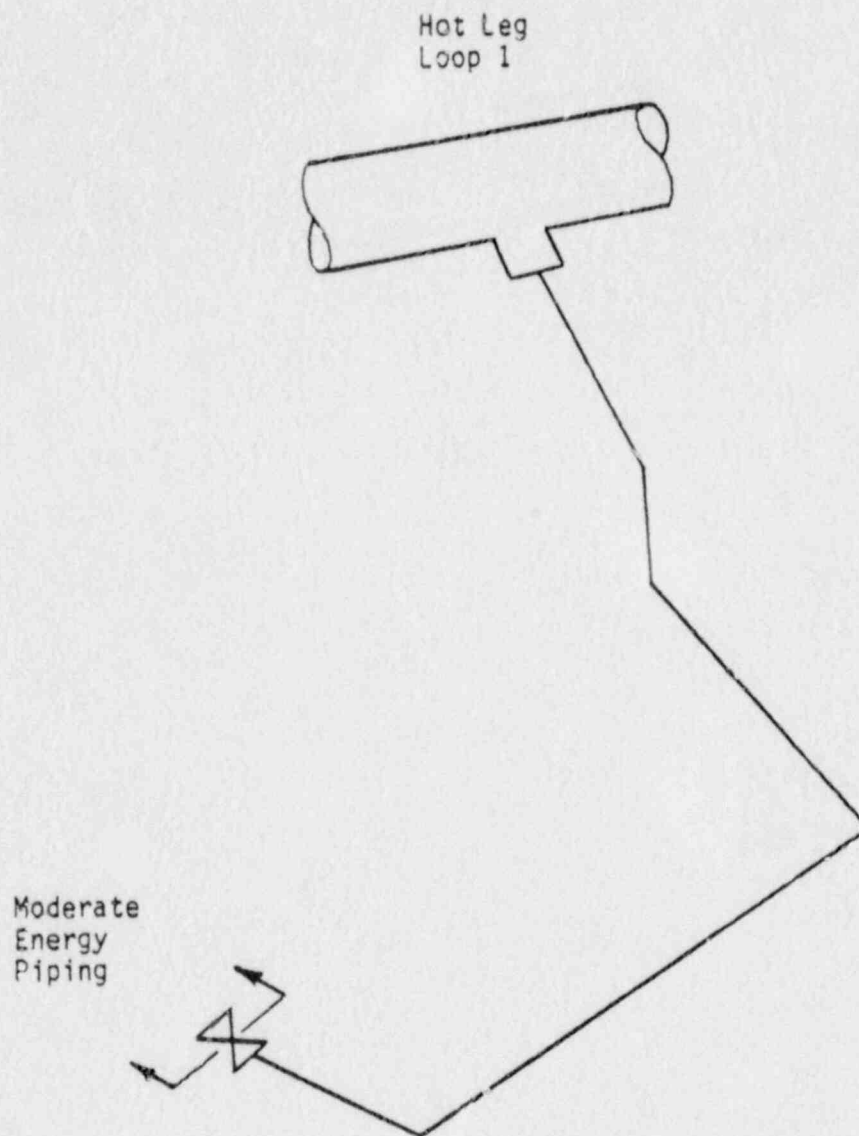
Figure 5-1   Schematic Layout of the RHR Lines - Loop 1, Units 1 and 2

Hot Leg
Loop 2

Node 135

Node 130E

Moderate
Energy
Piping
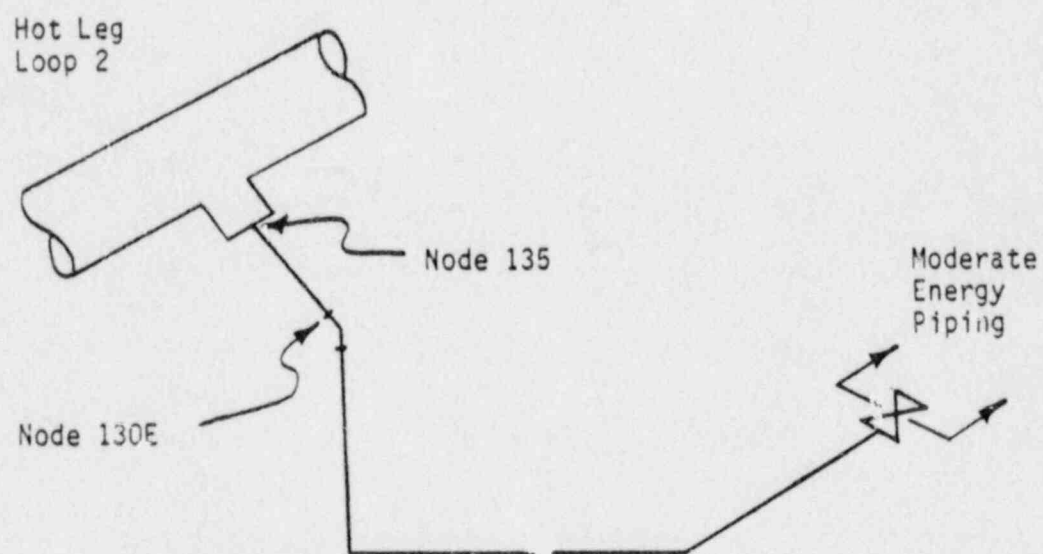
Figure 5-2 Schematic Layout of the RHR Lines - Loop 2, Units 1 and 2

Moderate
Energy
Piping

Hot Leg
Loop 3
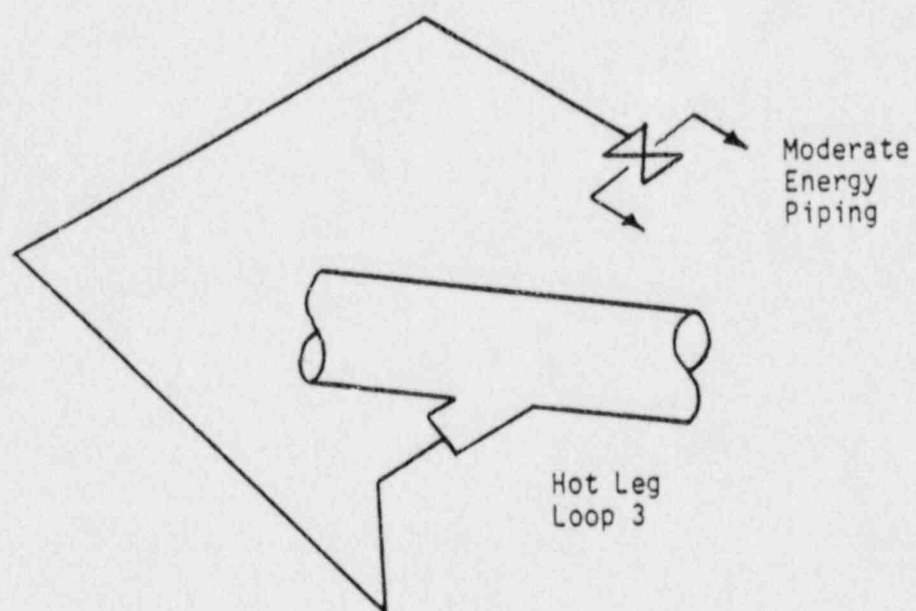
Figure 5-3.   Schematic Layout of RHR Lines Loop 3, Units 1 and 2

SECTION 6.0

FRACTURE MECHANICS EVALUATION

6.1 Global Failure Mechanism

Determination of the conditions which lead to failure in stainless steel should be done with plastic fracture methodology because of the large amount of deformation accompanying fracture. One method for predicting the failure of ductile material is the [ ]^{a,c,e} method, based on traditional plastic limit load concepts, but accounting for [
]^{a,c,e} and taking into account the presence of a flaw. The flawed pipe is predicted to fail when the remaining net section reaches a stress level at which a plastic hinge is formed. The stress level at which this occurs is called as the flow stress. [

]^{a,c,e} This methodology has been shown to be applicable to ductile piping through a large number of experiments and is used here to predict the critical flaw size in the RHR line. The failure criterion has been obtained by requiring equilibrium of the section containing the flaw (Figure 6-1) when loads are applied. The detailed development is provided in Appendix A for a through-wall circumferential flaw in a pipe with internal pressure, axial force, and imposed bending moments. The limit moment for such a pipe is given by:

[   ] a,c,e (6.1)

[   ]^{a,c,e} (6.2)

where:

[

]^{a,c,e}

[

$$\sigma_f = 0.5 (\sigma_y + \sigma_u) \text{ (flow stress)}$$

]^{a,c,e}

The analytical model described above accurately accounts for the piping internal pressure as well as imposed axial force as they affect the limit moment. Good agreement was found between the analytical predictions and the experimental results (reference 6-1). Flaw stability evaluations using this analytical model, are presented in section 6.3.

6.2 Leak Rate Predictions

The purpose of this section is to discuss the method which will be used to predict the flow through a postulated crack and present the leak rate calculation results for postulated through-wall circumferential cracks in the RHR line.

6.2.1 General Considerations

The flow of hot pressurized water through an opening to a lower back pressure (causing choking) is taken into account. For long channels where the ratio of the channel length, L, to hydraulic diameter, D_H, (L/D_H) is greater than [ ]^{a,c,e}, both [ ]^{a,c,e} must be considered. In this situation the flow can be described as being single-phase through the channel until the local pressure equals the saturation pressure of the fluid. At this point, the flow begins to flash and choking occurs. Pressure losses due to momentum changes will dominate for [ ]^{a,c,e} However, for large L/D_H values, friction pressure drop will become important and must be considered along with the momentum losses due to flashing.

6.2.2 Calculation Method

In using the isentropic equilibrium model, the basic method used in the leak rate calculations is the method developed by [

$]^{a,c,e}$.

The flow rate through a crack was calculated in the following manner. Figure 6-2 from reference 6-2 was used to estimate the critical pressure, Pc, for the primary loop enthalpy condition and an assumed flow. Once Pc was found for a given mass flow, the [$]^{a,c,e}$ was found from figure 6-3 taken from reference 6-2. For all cases considered, since [$]^{a,c,e}$ Therefore, this method will yield the two-phase pressure drop due to momentum effects as illustrated in figure 6-4. Now using the assumed flow rate, G, the frictional pressure drop can be calculated using

$$\Delta P_f = [\qquad\qquad]^{a,c,e} \qquad\qquad (6.3)$$

where the friction factor f is determined using the [$]^{a,c,e}$ The crack relative roughness, ε, was obtained from fatigue crack data on stainless steel samples. The relative roughness value used in these calculations was [$]^{a,c,e}$ RMS.

The frictional pressure drop using Equation 6.3 is then calculated for the assumed flow and added to the [
                $]^{a,c,e}$ to obtain the total pressure drop from the primary system to the atmosphere. Thus,

$$\text{Absolute Pressure} - 14.7 = [\qquad\qquad]^{a,c,e} \qquad (6.4)$$

for a given assumed flow G. If the right-hand side of equation 6.4 does not agree with the pressure difference between the piping under consideration and the atmosphere, then the procedure is repeated until equation 6.4 is satisfied to within an acceptable tolerance and this results in the flow value through the crack. This calculational procedure has been recommended by [

))]^{a,c,e} for this type of [

]^{a,c,e} calculation.

6.2.3 Leak Rate Calculations

Leak rate calculations were made as a function of postulated through-wall crack length for the critical location previously identified. The crack opening area was estimated using the method of reference 6-4 and the leak rates were calculated using the calculation methods described above. The leak rates were calculated using average material properties with the normal operating loads of axial force F = 196 kips and bending moment M = 395 in-kips.

The crack length yielding a leak rate of 10 gpm (10 times the leak detection requirement of 1.0 gpm) is found to be [   ]^{a,c,e}.

Thus the reference flaw size of [   ]^{a,c,e} is established.

6.2.4 Leak Detection Capability, Administrative Procedures and Technical Specification Requirements

All LBB candidate lines at South Texas Project are located inside the containment. The STP leakage detection criterion includes a detected unidentified leak rate of 1.0 gpm and, in accordance with NUREG-1061, Volume 3, a margin of 10 was applied to the leak rate to define the leakage size flaw used in the stability analysis. The basis for the 1.0 gpm leak rate is the presence (inside the containment) of diverse and redundant leakage detection systems to measure containment noble gas radioactivity, airborne particulate radioactivity, and containment sump level and flow rate. These systems are designed to alarm in the control room at a setpoint equivalent of less than or equal to 1 gpm. Indication of containment humidity is also provided in the

control room. These methods are in compliance with Regulatory Guide 1.45 as discussed in FSAR Subsection 5.2.5.

In addition to the above control room alarms and indications, Technical Specification 4.4.6.2.1 requires monitoring of containment gaseous or particulate radioactivity and normal sump inventory and discharge at least once per 12 hours. This section of the technical specification also requires performance of a reactor coolant system inventory balance at least once per 72 hours.

Detected leaks will be repaired within the system limiting conditions for operation established in either technical specifications or administrative procedures. When leakage is detected in reactor coolant pressure boundary piping, Technical Specification 3.4.6.2 requires that the plant be in hot standby within six hours and in cold shutdown within the next thirty hours. Repair would be required before restart.

Experience at other Westinghouse plants indicates a normal background unidentified average leakage rate of between 0.1 gpm and 0.3 gpm, and it has also been demonstrated with pressurized pipe tests that leak rates above 0.1 gpm at one location can be readily detected visually. The undefined leakage rate at STP is expected to be similar to other plants. Experience at similar plants and the results of these tests indicated that a 1.0 gpm leak rate can be reliably detected and located during plant operation.

6.3 Stability Evaluation Using the "Z" Factor Approach

A typical segment of the pipe under maximum loads of axial force F and bending moment M is schematically illustrated as shown in figure 6-5. In order to calculate the critical flaw size, a plot of the limit moment versus crack length is generated as shown in figure 6-6. The critical flaw size corresponds to the intersection of this curve and the maximum load line. The critical flaw size is calculated using the lower bound base metal tensile

properties established in section 4.0. From figure 6-6 the critical flaw size is seen to be [$]^{a,c,e}$ for the base metal.

The weld at the governing location is a field weld using a GTAW process. Other field welds on the RHR lines are either GTAW or SMAW. It has been established (reference 6-5) that GTAW welds exhibit superior toughness properties as compared to SMAW welds. For this evaluation, a "Z" factor correction for SMAW welds was conservatively applied even though the actual weld of interest is a GTAW weld.

The "Z" factor was applied (reference 6-5) as follows:

$$Z = 1.15 [1 + 0.013 (O.D. - 4)] \tag{6.5}$$

where OD is the outer diameter of the pipe in inches. Substituting OD = 12.75 inches, the Z factor was calculated to be 1.2808. The applied loads were increased by the Z factor and the plot of limit load versus crack length was regenerated as shown in figure 6-7. The lower bound base metal tensile properties (section 4.0) were used for this purpose. From figure 6-7, the critical flaw size is seen to be [$]^{a,c,e}$ long. Noting that the flaw yielding a leakage of 10 gpm (i.e. leakage size flaw) was calculated to be [$]^{a,c,e}$ long, a factor of 2.8 exists between the leakage size flaw and the critical flaw. Thus, a margin of greater than 2 on flaw size is in evidence.

In order to determine the margin on applied loads (normal plus SSE), the applied loads were increased by a factor of 1.79 (i.e. 1.4 Z) and the plot of limit load versus crack length was generated as shown in figure 6-8. Again the lower bound base metal tensile properties were used for this purpose. From figure 6-8 the critical flaw size is seen to be [$]^{a,c,e}$ long which is larger than the [$]^{a,c,e}$ inches long leakage size flaw. Thus a margin on load of at least 1.4 times normal plus SSE loads is demonstrated.

6.4 Local Stability Analysis

In this section the local stability analysis is performed to show that unstable crack extension will not result when postulated through wall flaws are subjected to maximum plant loads.

At the critical location identified in section 5.0, the (normal plus SSE) outer surface axial stress; σ_a, is seen to be 13.9 ksi based on the minimum wall thickness. The (normal plus SSE) axial force and bending moment are F = 198 kips and M = 862 in-kips.

The minimum yield strength for flaw stability analysis is [   ]^{a,c,e} ksi (see section 4). The EPRI elastic-plastic fracture handbook method is used to calculate the $J_{applied}$ using the normal plus SSE loads. The $J_{applied}$ was calculated for a [   ]^{a,c,e} long postulated through wall flaw (which is 2 times the reference flaw size) and was found to be [   ]^{a,c,e} which is lower than J_{Ic} of 959 in-lb/in^2.

In addition, for a leakage size flaw, i.e. the reference flaw [   ]^{a,c,e} long, the normal plus SSE load was increased by a factor of $\sqrt{2}$. The J-T analysis gave an applied J of [   ]^{a,c,e} which is also less than J_{Ic} of 959 in-lb/in^2. Thus crack stability is demonstrated for both the above cases.

6.5 References

6-1 Kanninen, M. F. et al., "Mechanical Fracture Predictions for Sensitized Stainless Steel Piping with Circumferential Cracks" EPRI NP-192, September 1976.

6-2 [

                                        ]^{a,c,e}

6-3 [
     ]^{a,c,e}.

6-4 Tada, H., "The Effects of Shell Corrections on Stress Intensity Factors and the Crack Opening Area of Circumferential and a Longitudinal Through-Crack in a Pipe," Section II-1, NUREG/CR-3464, September 1983.

6-5 ASME Code Section XI, Winter 1985 Addendum, Article IWB-3640.

a,c,e
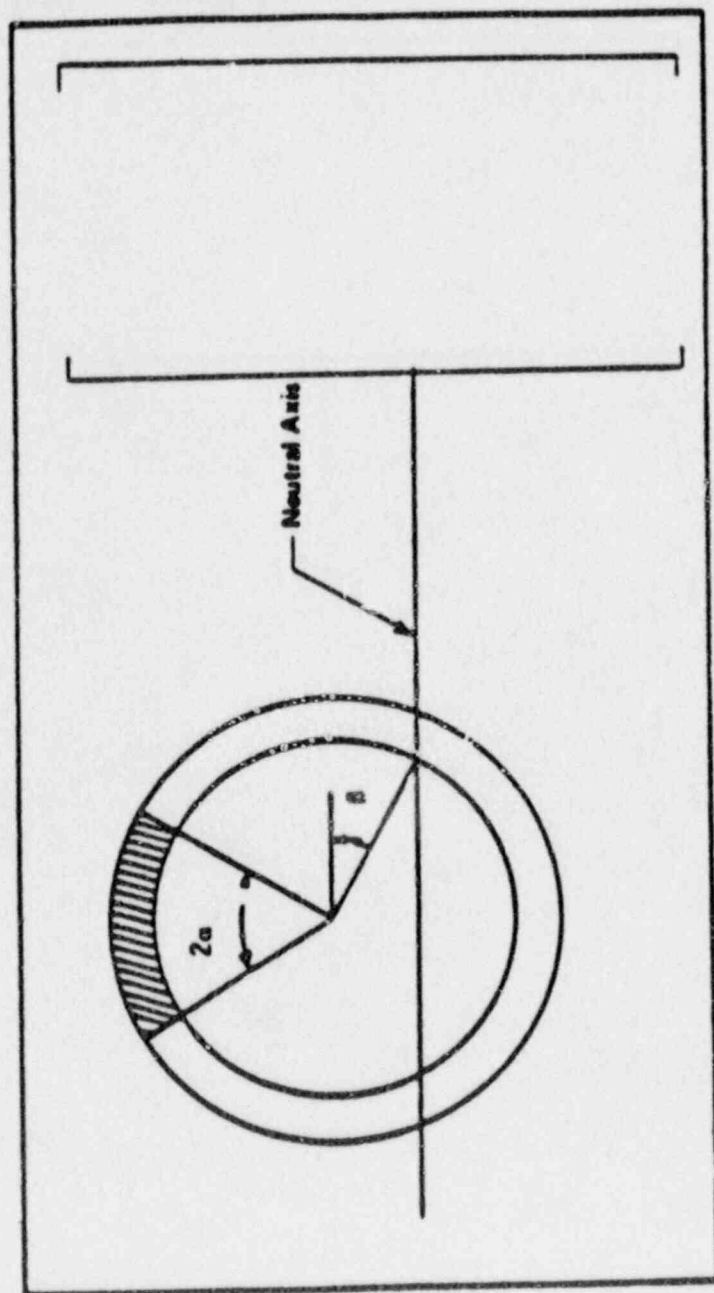
Figure 6-1 [   ]a,c,e stress distribution

MASS VELOCITY (lb/(sec)(in²))

a,c,e

Figure 6-2. Analytical Predictions of Critical Flow Rates of Steam-Water
Mixtures

CRITICAL PRESSURE RATIO (p$_c$/p$_o$)

a,c,e

LENGTH/DIAMETER RATIO (L/D)

Figure 6-3 [   ]^{a,c,e} Pressure Ratio as a Function of L/D
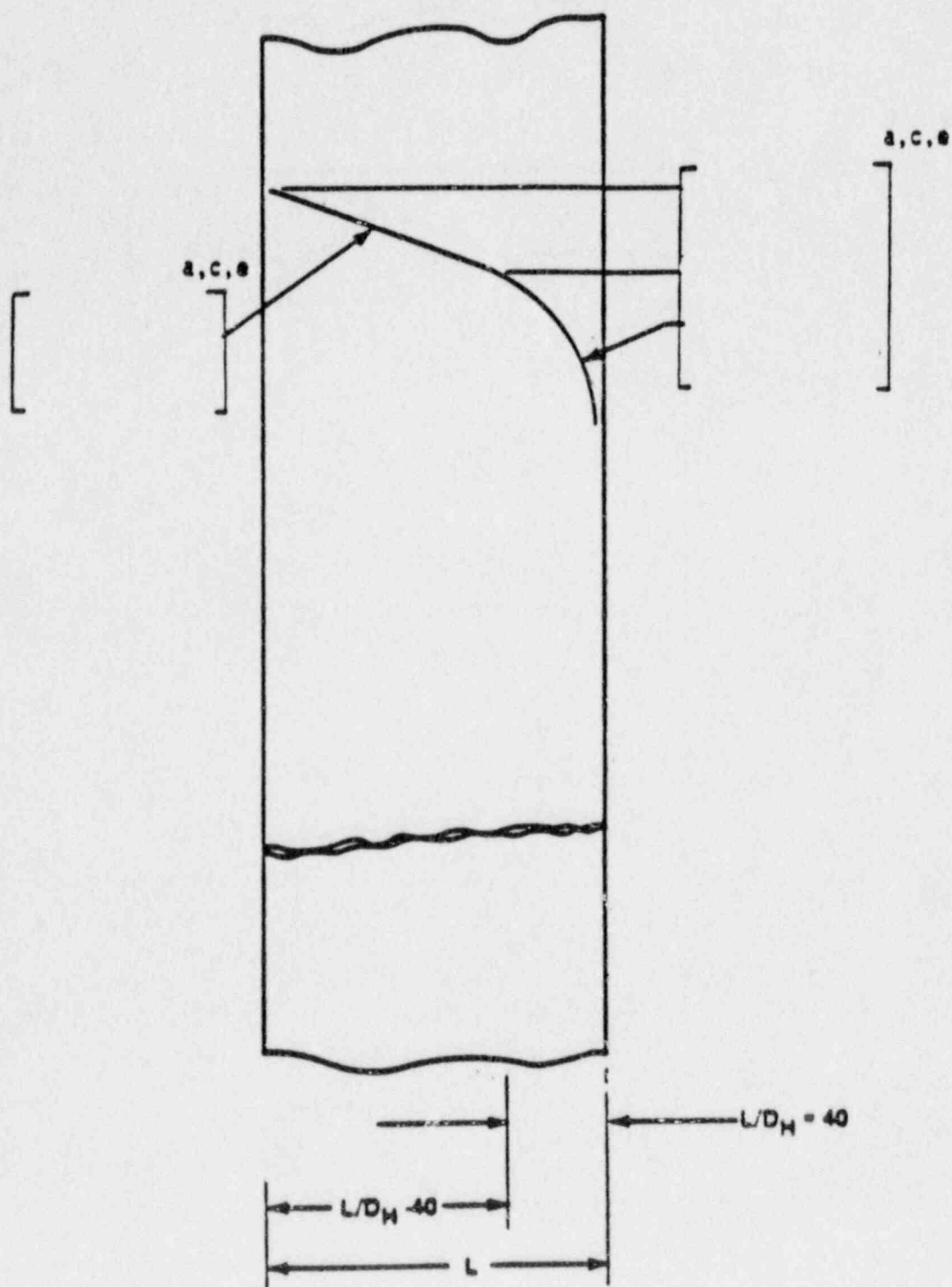
Figure 6-4 Idealized Pressure Drop Profile Through a Postulated Crack
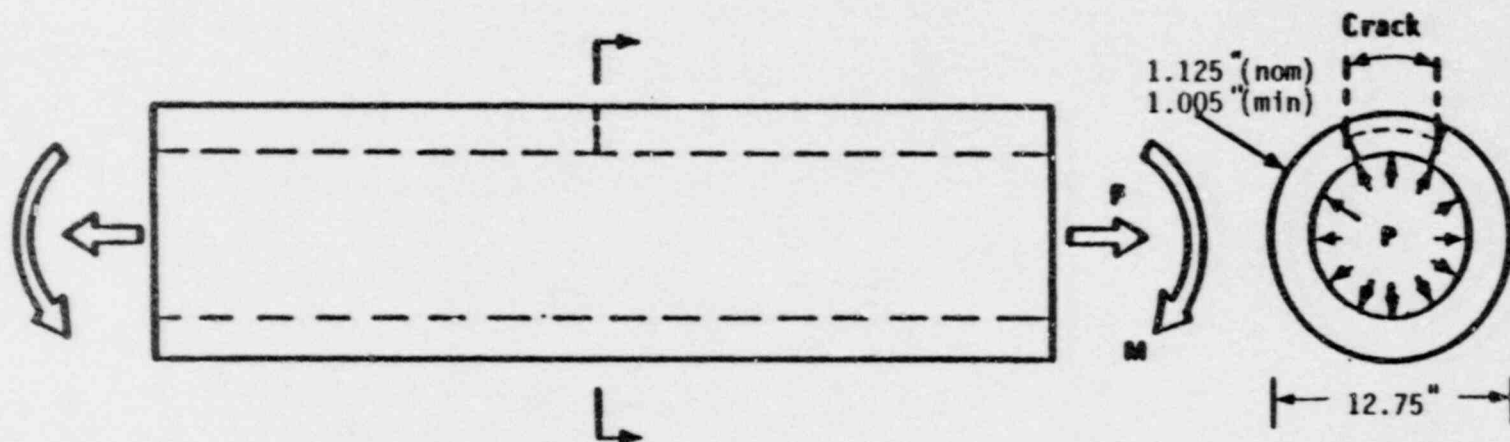
P = 2235 psi
F = 198 kips
M = 862 in-kips

Figure 6-5 Loads Acting on the Pipe Model at the Governing Location

a,c,e

OD = 12.75"
t = 1.005"
P = 2235 psig
F = 198 kips
σ_y = 22.1 ksi
σ_u = 66.4 ksi
σ_F = 44.3 ksi
Temp = 623°F
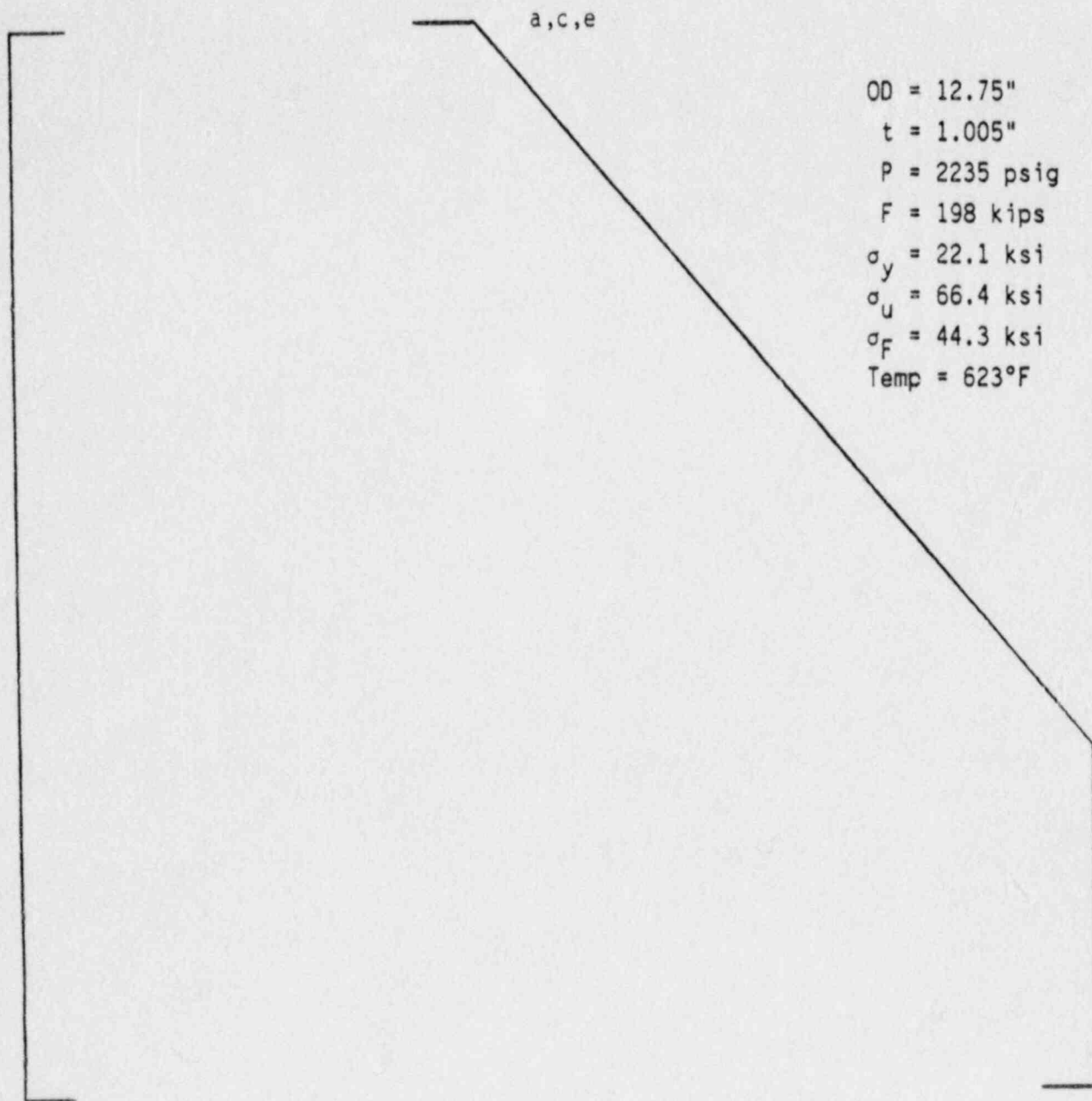
Figure 6-6. Critical Flaw Size Prediction for the Base Metal Using
Limit Load Approach

6-14

a,c,e

OD = 12.75"
t = 1.005"
P = 2235 psig
F* = 254 kips
σ_y = 22.1 ksi
σ_u = 66.4 ksi
σ_F = 44.3 ksi
Temp = 623°F
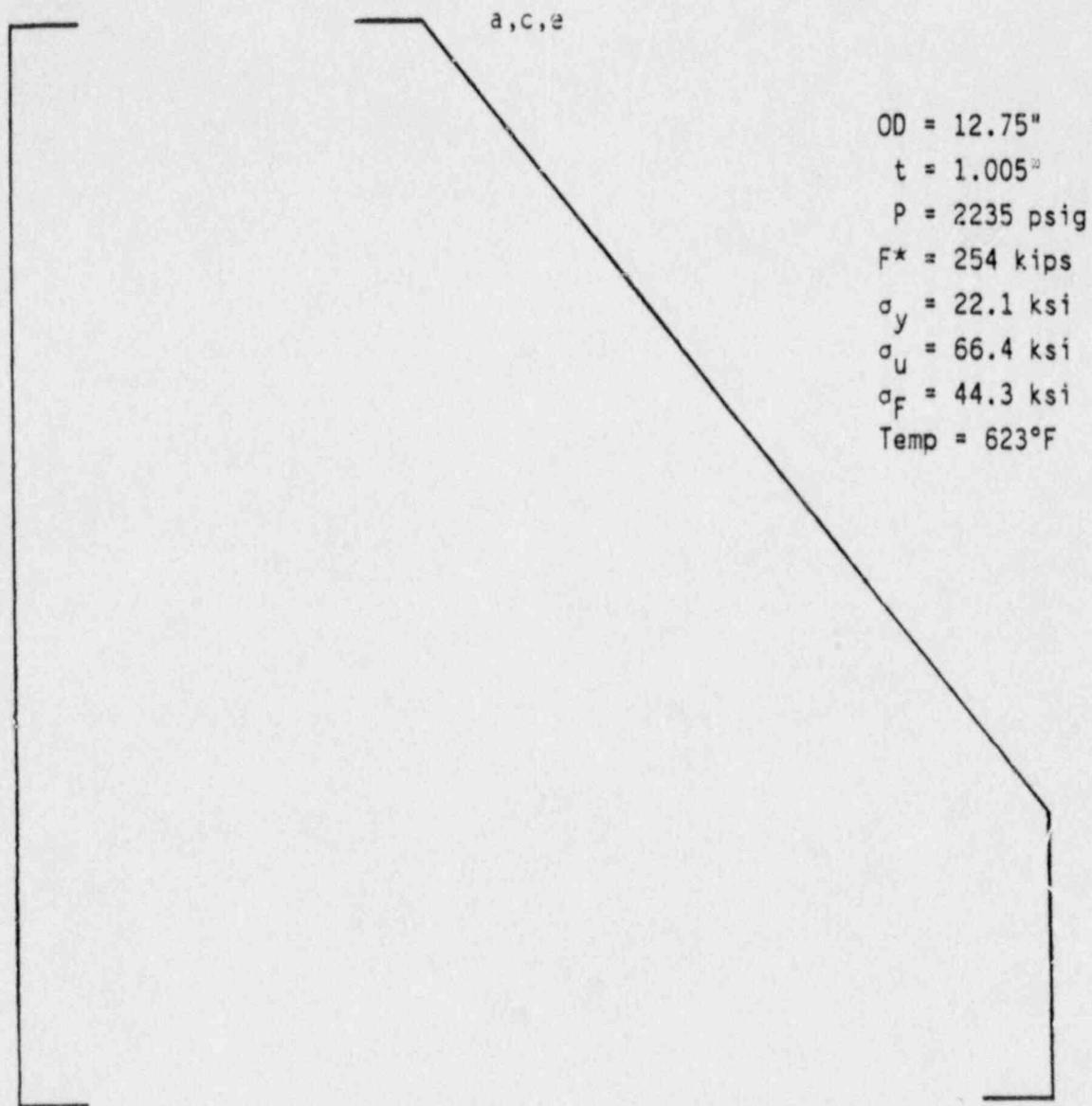
*Z Factor of 1.28 was applied to the load resulting in applied force of 254 kips.

Figure 6-7 Z-Factor Calculations for SMAW Welds to Demonstrate Margin on Flaw Size

a,c,e

OD = 12.75"
τ = 1.005"
P = 2235 psig
F* = 354 kips
σ_y = 22.1 ksi
σ_u = 66.4 ksi
σ_F = 44.3 ksi
Temp = 623°F
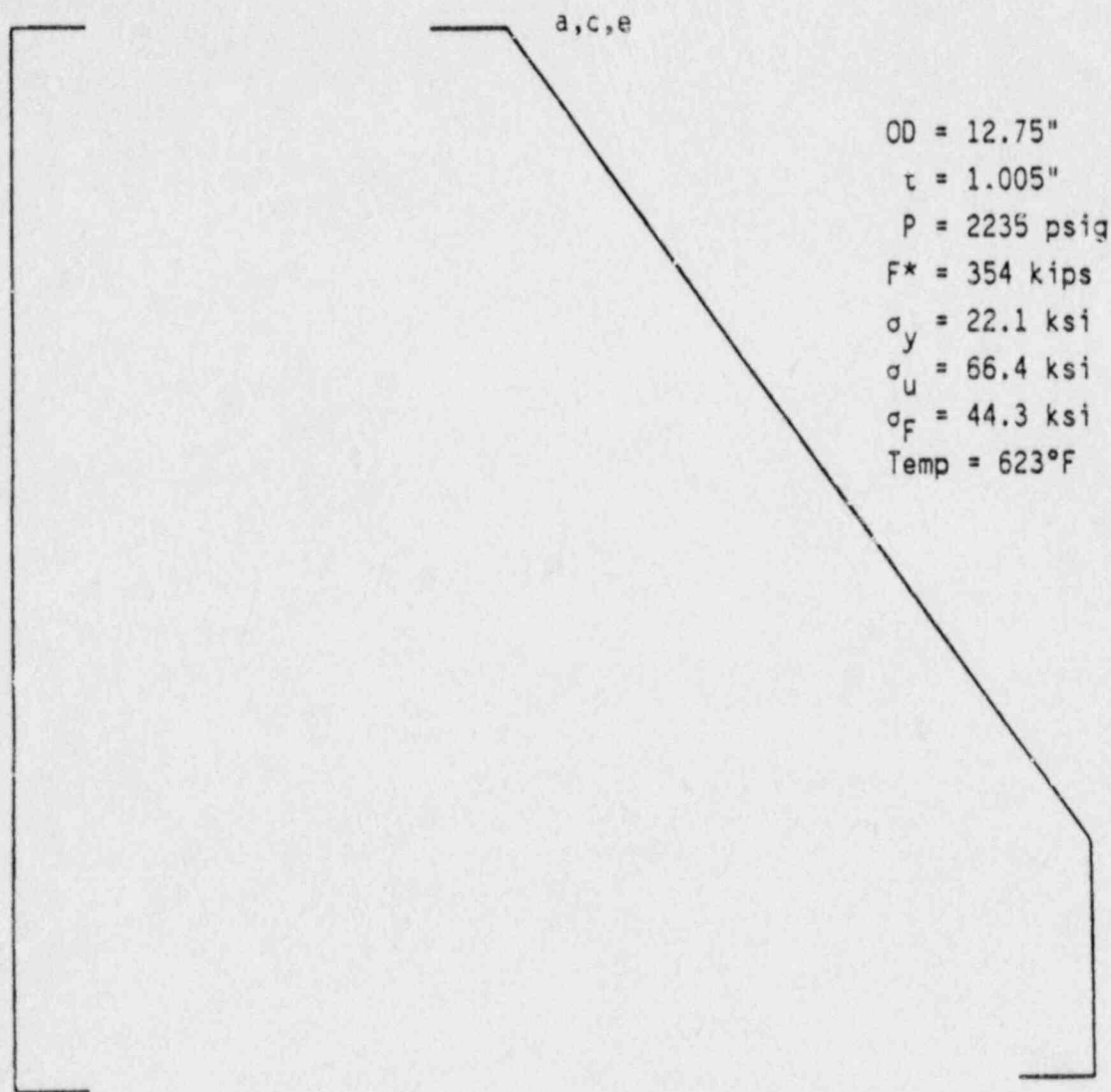
*$\sqrt{2}$ Z Factor of 1.79 was applied to the load. THis resulted in applied force of 354 kips.

Figure 6-8 $\sqrt{2}$ Z-Factor Calculations for SMAW Welds to Demonstrate Margin on Loads
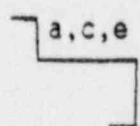
SECTION 7.0

ASSESSMENT OF FATIGUE CRACK GROWTH

The fatigue crack growth on the South Texas Project RHR line was determined by comparison with a generic fatigue crack growth analysis of a similar piping system. The details of the generic fatigue crack growth analysis are presented in Appendix B. By comparing all parameters critical to the fatigue crack growth analysis, between STP Units 1 and 2 RHR lines and generic RHR lines, it was concluded that the generic analysis would envelop the fatigue crack growth of the STP RHR lines.

Due to similarities in Westinghouse PWR designs it was possible to perform a generic fatigue crack growth calculation which would be applicable to many projects. A comparison was made of stresses and number of cycles, material, geometry, and types of discontinuities.

The following summarizes the parameters which were compared:

	$\big[$ $\big]$ a,c,e	$\big[$ $\big]$ a,c,e
<u>Critical Location</u>		
Pipe Outer Diameter	12.75"	12.75"
Thickness	1.005"	1.005"
Material	Austenitic Stainless Steel	Austenitic Stainless Steel
Normal Temperature	617°F	623°F
Normal Pressure	2235 psig	2235 psig
Normal Operating Stress (Press, DW, Thermal Exp.)	20.3 ksi	9.2 ksi
Thermal Transients	See Appendix B	*

* Thermal transient loadings are nearly identical for the two projects.

This comparison demonstrates the many similarities between the STP RHR line and the generic RHR line evaluation. The normal operating stress for the STP RHR lines is significantly lower. This will result in reduced crack growth.

7.1 Acceptability of Fatigue Crack Growth

A detailed discussion pertaining to the fatigue crack growth law used in the analysis described in Appendix B and the data used in defining the law are provided in reference (7-1). For the assessment of crack growth acceptability, the crack growth results of the generic analysis presented in appendix B are used conservatively and are considered applicable to the STP RHR lines. Detailed discussion in support of this assumption has been provided in the previous section.

The maximum allowable preservice indication may have a depth of 0.1 in. per IWB-3514.3, Allowable Indication Standard for Austenitic Piping, ASME Code, Section XI - Division 1, 1986 edition. From the generic analysis described in Appendix B, the final flaw size (40 year life) will be 0.1514 in. for a postulated initial flaw size of 0.15 in. subjected to the design transients.
[

]a,c,e Thus, the first
criterion on flaw depth is satisfied.

Secondly, the worst case transient ΔK value for the maximum crack depth is
[   ]a,c,e The flow stress for the base metal at 623°F is 44.3 ksi which can be used to obtain a conservative estimate of the plastic zone size.

The expression for the plastic zone size, r_p, calculation is: (reference 7-2)

$$r_p = \frac{\pi}{32} \left(\frac{\Delta K}{\sigma_f}\right)^2$$

From the preceding equation, the plastic zone size is calculated to be [
]^{a,c,e} The remaining ligament for the 0.1514 in. deep end-of-fatigue-life flaw
is 0.854 in. (i.e. 1.005 - 0.1514). Thus, the plastic zone size is far less
than the remaining ligament.

Based on the above, it is concluded that for the STP RHR Lines, the fatigue
crack growth during service will not be significant.

7.2 References

7-1 Bamford, W. H. "Fatigue Crack Growth of Stainless Steel Reactor Coolant
     Piping in a Pressurized Water Reactor Environment," ASME Trans. Journal
     of Pressure Vessel Technology, February 1979.

7-2 Rice, J. R., ASTM STP, 1967, Volume 415, p. 247.

SECTION 8.0

ASSESSMENT OF MARGINS

In the preceding sections, the leak rate calculations, fracture mechanics analysis and fatigue crack growth assessment were performed. Margins at the critical location are summarized below:

In section 6.3 the "critical" flaw size using the limit load method is calculated to be [   ]^{a,c,e} long. Using the IWB-3640 approach (i.e. "Z" factor approach), the critical flaw size at the governing location weld is found to be [   ]^{a,c,e} long. In section 6.4 it is demonstrated, using the J-T approach that a postulated [   ]^{a,c,e} long through-wall flaw will remain stable when subjected to normal plus SSE loads. Based on the above, the critical flaw size will exceed [   ].^{a,c,e}

In section 6.2 it is shown that at the critical location, a flaw of [   ]^{a,c,e} would yield a leak rate of 10 gpm. Thus, there is a margin of at least 2 on flaw size and a margin of 10 with respect to the plant leak detection capability of 1 gpm.

In sections 6.3 and 6.4 it is shown that the reference flaw [   ]^{a,c,e} yielding a leak rate of 10 gpm would be stable when subjected to a load equal to 1.4 (normal + SSE). Specifically, using the IWB-3640 approach (section 6.3) a [   ]^{d,c,e} long through-wall flaw was shown to be stable when subjected to 1.4 Z (normal + SSE) loads. Also, based on the local stability analysis (section 6.4) the leakage size flaw of [   ]^{a,c,e} inches was shown to be stable when subjected to $\sqrt{2}$ (normal + SSE) loads.

In summary, relative to

1. Loads

   The leakage-size crack will not experience unstable crack extension even
   if very large loads of $\sqrt{2}$ (normal plus SSE) are applied.

2. Flaw Size

   a. A margin of at least 2 exists between the critical flaw and the flaw
      yielding a leak rate of 10 gpm.

   b. If limit load is used as the basis for critical flaw size, an even
      larger margin would result.

3. Leak Rate

A margin of 10 exists for the reference flaw [   ]^{a,c,e} between
calculated leak rate and the 1 gpm leak detection criteria of Regulatory Guide
1.45.

A summary comparison of criteria and analytical results is given in table
8-1. The criteria are seen to be met.

TABLE 8-1
COMPARISON OF RESULTS VS. CRITERIA

CRITERION	RESULT
1. NUREG 1061 Volume 3 Section 5.2(h) - Margin on Flaw Size	Met (Required margin of 2 demonstrated)
2. NUREG 1061 Volume 3 Section 5.2(i) - Margin on Load	Met (Required margin of $\sqrt{2}$ demonstrated)
3. NUREG 1061 Volume 3 Section 5.7 - Margin on Leak Rate	Met (Margin of 10 on leak rate demonstrated)
4. NRC criteria on allowable fatigue crack growth	Met (a_f < 60% wall thickness and plastic zone size < remaining ligament)

SECTION 9.0

CONCLUSIONS

This report justifies the elimination of RHR line pipe breaks from the structural design basis for the South Texas Units 1 and 2 as follows:

a. Stress corrosion cracking is precluded by use of fracture resistant materials in the piping system and controls on reactor coolant chemistry, temperature, pressure, and flow during normal operation.

b. Water hammer should not occur in the RCS piping (primary loop and the attached auxiliary lines) because of system design, testing, and operational considerations.

c. The effects of low and high cycle fatigue on the integrity of the RHR line piping are negligible.

d. Ample margin exists between the leak rate of small stable flaws and the requirements of Reg. Guide 1.45. The STP system for detecting unidentified leaks in the RCS conforms to the requirements of Reg. Guide 1.45 (FSAR section 5.2.5)

e. Ample margin exists between the small stable flaw sizes of item d and the critical flaw.

f. With respect to stability of the reference flaw, ample margin exists between the maximum postulated loads and the plant specific as-built faulted loads (i.e. normal + SSE).

The reference flaw will be stable because of the ample margins in d, e, and f and will leak at a detectable rate which will assure a safe plant shutdown.

Based on the above, it is concluded that pipe breaks in the RHR piping need not be considered in the structural design basis of South Texas Project Units 1 and 2.

APPENDIX A

LIMIT MOMENT

[

] a,c,e

a,c,

Figure A-1   Pipe with a Through-Wall Crack in Bending

APPENDIX B

FATIGUE CRACK GROWTH CONSIDERATION

B.1 Thermal Transient Stress Analysis

The thermal transient stress analysis was performed for a typical PWR plant to obtain the through wall stress profiles for use in the fatigue crack growth analysis of Section B.2. The through wall stress distribution for each transient was calculated for i) the time corresponding to the maximum inside surface stress and, ii) the time corresponding to the minimum inside surface stress. These two stress profiles are called the maximum and minimum through wall stress distribution, respectively, for convenience. The constant stresses due to pressure, deadweight and thermal expansion (at normal operating temperature, 617°F) loadings were superimposed on the through wall cyclical stresses to obtain the total maximum and minimum stress profile for each transient. Linear through wall stress distributions were calculated by conservative simplified methods for all transients.

B.1.1 Critical Location for Fatigue Crack Growth Analysis

The RHR line design thermal transients (Section B.1.2), 1-D analysis data on RHR line thermal transient stresses (based on ASME Section III NB-3600 rules) and the geometry were reviewed to select the worst location for the fatigue crack growth analysis. [
determined to be the most critical location for the fatigue crack growth
]^{a,c,e} This location is selected as the worst location based on the following considerations:

i)   the fatigue usage factor is highest.
ii) the effect of discontinuity due to undercut at weld will tend to increase the cyclical thermal transient loads.
iii) the review of data shows that the 1-D thermal transient stresses in the RHR line piping section are generally higher near the [
                                                        ]^{a,c,e}

B.1.2 Design Transients

The transient conditions selected for this evaluation are based on conser-
vative estimates of the magnitude and the frequency of the temperature
fluctuations resulting from various operating conditions in the plant. These
are representative of the conditions which are considered to occur during
plant operation. The fatigue evaluation based on these transients provides
confidence that the component is appropriate for its application over the
design life of the plant. All the normal operating and upset thermal
transients, in accordance with the design specification and the applicable
system design criteria document (B-1), were considered for this evaluation.
Out of these, [

$$]^{a,c,e}$$

B.1.3 Simplified Stress Analysis

The simplified analysis method was used to develop conservative maximum and
minimum linear through wall stress distributions due to thermal transients.
[

$]^{a,c,e}$ The inside surface stress was calculated by the following
equation which is similar to the transient portion of ASME Section III
NB-3600, Eq. 11:

$$S_i = [\qquad\qquad\qquad)]^{a,c,e} \qquad (B.1)$$

where,

S_i = inside surface stress

$$\left[\qquad\qquad\qquad \right]^{a,c,e} \qquad (B.2)$$

$$(B.3)$$

[┐ a,c,e

                                                                                           ┘

[

                                              ]a,c,e The maximum and minimum inside
surface stresses were searched from the S_i values calculated for each time
step of the transient solution.

The outside surface stresses corresponding to maximum and minimum inside
stresses were calculated by the following equations:

S_{01} = [   ] a,c,e   (B.5)

S_{02} = [   ] a,c,e   (B.6)

where,

                                                                                       ┐ a,c,e
[

                                                                                       ┘

B-3

The material properties for the RHR pipe [   )]^{a,c,e} and the RCL
[

]^{a,c,e} The values of E and α, at the normal operating temperature,
provide a conservative estimation of the through wall thermal transient
stresses as compared to room temperature properties. The following values
were conservatively used, which represent the highest of the [
]^{a,c,e} materials:

$$\left[\right]^{a,c,e}$$

The maximum and minimum linear through wall stress distribution for each
thermal transient was obtained by [
]^{a,c,e} The simplified analysis
discussed in this section was performed for all thermal transients of table
B-1. The inside and outside surface stresses calculated by simplified methods
for the transients are shown in table B-2.

B.1.4 OBE Loads

The stresses due to OBE loads were neglected in the fatigue crack growth
analysis since these loads are not expected to contribute significantly to
crack growth due to the small number of cycles.

B.1.5 Total Stress for Fatigue Crack Growth

The total through wall stress at a section was obtained by superimposing the
pressure load stresses and the stresses due to deadweight and thermal
expansion (normal operating case) on the thermal transient stresses (of table
B-2). Thus, the total stress for fatigue crack growth at any point is given
by the following equation:

Total Stress		Thermal		Stress Due		Stress	
for		Transient		to		Due to	
Fatigue	=	Stress	+	DW +	+	Internal	(B.7)
Crack Growth				Thermal		Pressure	
				Expansion			

The envelope normal loads from thermal expansion, deadweight and pressure for calculating the total stresses of equation B.7 are summarized in table B-3.

B.2 Fatigue Crack Growth Analysis

The fatigue crack growth analysis was performed to determine the effect of the design thermal transients, in table B-1. The analysis was performed for the critical cross section of the model which is identified in figure B-1. A range of crack depths was postulated, and each was subjected to the transients in table B-1, and envelope normal loads in table B-3.

B.2.1 Analysis Procedure

The fatigue crack growth analyses presented herein were conducted in the same manner as suggested by Section XI, Appendix A of the ASME Boiler and Pressure Vessel Code. The analysis procedure involves assuming an initial flaw exists at some point and predicting the growth of that flaw due to an imposed series of stress transients. The growth of a crack per loading cycle is dependent on the range of applied stress intensity factor ΔK_I, by the following relation:

$$\frac{da}{dN} = Co\Delta K_I^n \qquad (B.2.1)$$

where "Co" and the exponent "n" are material properties, and ΔK_I is defined later, in equation (B.2.3). For inert environments these material properties are constants, but for some water environments they are dependent on the level of mean stress present during the cycle. This can be accounted

for by adjusting the value of "Co" and "n" by a function of the ratio of minimum to maximum stress for any given transient, as will be discussed later. Fatigue crack growth properties of stainless steel in a pressurized water environment have been used in the analysis.

The input required for a fatigue crack growth analysis is basically the information necessary to calculate the parameter ΔK_I, which depends on crack and structure geometry and the range of applied stresses in the area where the crack exists. Once ΔK_I is calculated, the growth due to that particular cycle can be calculated by equation (B.2.1). This increment of growth is then added to the original crack size, the ΔK_I adjusted, and the analysis proceeds to the next transient. The procedure is continued in this manner until all the transients have been analyzed.

The crack tip stress intensity factors (K_I) to be used in the crack growth analysis were calculated using an expression which applies for a semi-elliptic surface flaw in a cylindrical geometry (reference B-3).

The stress intensity factor expression was taken from Reference B-3 and was calculated using the actual stress profiles at the critical section. The maximum and minimum stress profiles corresponding to each transient were input, and each profile was fit by a third order polynomial:

$$\sigma(x) = A_0 + A_1 \frac{x}{t} + A_2 \left(\frac{x}{t}\right)^2 + A_3 \left(\frac{x}{t}\right)^3 \qquad (B.2.2)$$

The stress intensity factor $K_I(\phi)$ was calculated at the deepest point of the crack using the following expression:

$$\left[\right]^{a,c,e} \qquad (B.2.3)$$

B-6

$$\begin{bmatrix} & & & \\ & & & \\ & & & \\ & & & \\ & & & \\ & & & \end{bmatrix}^{a,c,e}$$

Calculation of the fatigue crack growth for each cycle was then carried out using the reference fatigue crack growth rate law determined from consideration of the available data for stainless steel in a pressurized water environment. This law allows for the effect of mean stress or R ratio (K_{Imin}/K_{Imax}) on the growth rates.

The reference crack growth law for stainless steel in a pressurized water environment was taken from a collection of data (B-4) since no code curve is available, and it is defined by the following equation:

$$\frac{da}{dN} = [\qquad\qquad\qquad\qquad]^{a,c,e} \quad (B.2.4)$$

where $K_{eff} = (K_{Imax}) (1-R)^{1/2}$

$$R = \frac{K_{Imin}}{K_{Imax}}$$

$\frac{da}{dN}$ = crack growth rate in micro-inches/cycle

B.2.2 Results

Fatigue crack growth analyses were carried out for the critical cross section. Analysis was completed for a range of postulated flaw sizes oriented circumferentially, and the results are presented in Table B-4. The postulated flaws are assumed to be six times as long as they are deep. Even for the largest postulated flaw of [
$]^{a,c,e}$ the result shows that the flaw growth through the wall will not occur during the 40 year design life of the plant. For smaller flaws, the flaw growth is significantly lower. For example, a postulated [$]^{a,c,e}$ inch deep flaw will grow less than [$]^{a,c,e}$. These results also confirm operating plant experience.

B.3 REFERENCES

B-1 Westinghouse System Standard Design Criteria 1.3, "Nuclear Steam Supply System Design Transients," Revision 2, April 15, 1974, Westinghouse Proprietary.

B-2 ASME Section III, Division 1-Appendices, 1983 Edition, July 1, 1983.

B-3 McGowan, J. J. and Raymund, M., "Stress Intensity Factor Solutions for Internal Longitudinal Semi-Elliptical Surface Flaws in a Cylinder Under Arbitrary Loadings", Fracture Mechanics ASTM STP 677, 1979, pp. 365-380.

B-4 Bamford, W. H., "Fatigue Crack Growth of Stainless Steel Reactor Coolant Piping in a Pressurized Water Reactor Environment", ASME Trans. Journal of Pressure Vessel Technology, February 1979.

TABLE B-1

THERMAL TRANSIENTS CONSIDERED FOR FATIGUE CRACK GROWTH EVALUATION

Trans. No.	Description	No. of Occurrences
		a,c,e

TABLE B-2
TRANSIENT STRESSES FOR RHR LINE
(psi)

Transient No.	Maximum Inside Stress	Corresponding Outside Stress	Minimum Inside Stress	Corresponding Outside Stress	
					a,c,e

TABLE B-3

ENVELOPE NORMAL LOADS

Condition

$$\left[\qquad\qquad\qquad\qquad \right]^{a,c,e}$$

Normal Operating

TABLE B-4

RHR LINE FATIGUE CRACK GROWTH RESULTS

Section Thickness [   ]* a,c

INITIAL CRACK	CRACK DEPTH AFTER YEAR			
DEPTH (in)	10	20	30	40

[   ] a,c,e

*This is conservatively taken as minimum thickness of the counter
bore region

a,c,e

RHR PIPE

Figure B-1 Schematic of RHR Line At [   ] a,c,e